Environmental Research 298 (2026) 124252

Contents lists available at ScienceDirect

Environmental Research

journal homepage: www.elsevier.com/locate/envres

Cytogenotoxic effects of polycyclic aromatic hydrocarbons complex mixture in human peripheral blood, lung A549 and liver HepG2 cells: Translation of a real-scenario exposure to *in vitro*

Luka Kazensky [a], Marija Jelena Lovrić Štefiček [b], Vilena Kašuba [a], Matjaž Novak [c], Karolina Belingar [c], Katarina Matković [a], Marko Gerić [a], Jasmina Rinkovec [b], Ivana Jakovljević [b], Katarina Baralić [e], Danijela Đukić-Ćosić [e], Mirta Milić [a], Želimir Jelčić [f,1], Gordana Pehnec [b], Bojana Žegura [c,d,*], Goran Gajski [a,**]

[a] Division of Toxicology, Institute for Medical Research and Occupational Health, 10000, Zagreb, Croatia
[b] Division of Environmental Hygiene, Institute for Medical Research and Occupational Health, 10000, Zagreb, Croatia
[c] Department of Genetic Toxicology and Cancer Biology, National Institute of Biology, 1000, Ljubljana, Slovenia
[d] Biotechnical Faculty, University of Ljubljana, 1000, Ljubljana, Slovenia
[e] Department of Toxicology "Akademik Danilo Soldatović", Faculty of Pharmacy, University of Belgrade, 11000, Belgrade, Serbia
[f] TAPI R&D, PLIVA Croatia Ltd., 10000, Zagreb, Croatia

ARTICLE INFO

Keywords:
Cytotoxicity
Genomic instability
In silico
Indoor air pollution
Public health

ABSTRACT

Polycyclic aromatic hydrocarbons (PAHs) are ubiquitous air pollutants, where their genotoxic potential raises significant public health concerns. This study evaluated the cytotoxic and genotoxic effects of an environmentally relevant mixture of 11 PAHs measured in indoor air from Zagreb households. Biological responses were assessed in three human-derived models: peripheral blood cells (PBCs), lung epithelial cells (A549), and liver carcinoma cells (HepG2). Short-term exposure scenarios were designed to mimic indoor inhalation over 1, 8, and 16 h, with treatments lasting 4 or 24 h. Cytotoxicity was evaluated via acridine orange/ethidium bromide staining in PBCs and the MTT assay in A549 and HepG2 cells, while genotoxicity was assessed using the alkaline comet and cytokinesis-block micronucleus assays. Overall, A549 and HepG2 cells displayed nonsignificant cyto- and genotoxic responses across all concentrations and exposure durations. In contrast, PBCs exhibited statistically significant, time- and concentration-dependent cytotoxicity. Genotoxic analyses revealed a biologically relevant, though statistically non-significant, threefold increase in micronuclei formation at the highest PAHs concentration after 4 h. A statistically significant increase in nucleoplasmic bridges was observed at the medium (8-h) concentration after 24 h, compared with controls. The limited biological responses align with the mixture's low toxic- (TEF) and genotoxic equivalency factor (GEF)-weighted toxicity derived from literature values, as the most abundant PAHs were low-potency compounds. Accordingly, under the experimental conditions applied, exposure did not result in detectable DNA or chromosomal damage. *In silico* analysis indicated that the mixture's toxicity is largely driven by the AHR–CYP–NQO1 axis.

1. Introduction

Air pollution remains a pressing global concern, with profound implications for both human and environmental health. Among the complex mixture of airborne contaminants, polycyclic aromatic hydrocarbons (PAHs), particulate matter (PM), volatile organic compounds (VOCs), toxic metals, and biological agents are commonly identified as major pollutants (Choi H et al., 2010; Kazensky et al., 2024; Lelieveld et al., 2023). PAHs represent a diverse group of organic compounds generated through both natural and anthropogenic

* Corresponding author. National Institute of Biology, Department of Genetic Toxicology and Cancer Biology, Večna pot 121, 1000, Ljubljana, Slovenia.
** Corresponding author. Institute for Medical Research and Occupational Health, Division of Toxicology, Ksaverska cesta 2, 10000 Zagreb, Croatia.
E-mail addresses: bojana.zegura@nib.si (B. Žegura), ggajski@imi.hr (G. Gajski).
[1] retired.

https://doi.org/10.1016/j.envres.2026.124252
Received 20 December 2025; Received in revised form 11 February 2026; Accepted 9 March 2026
Available online 14 March 2026

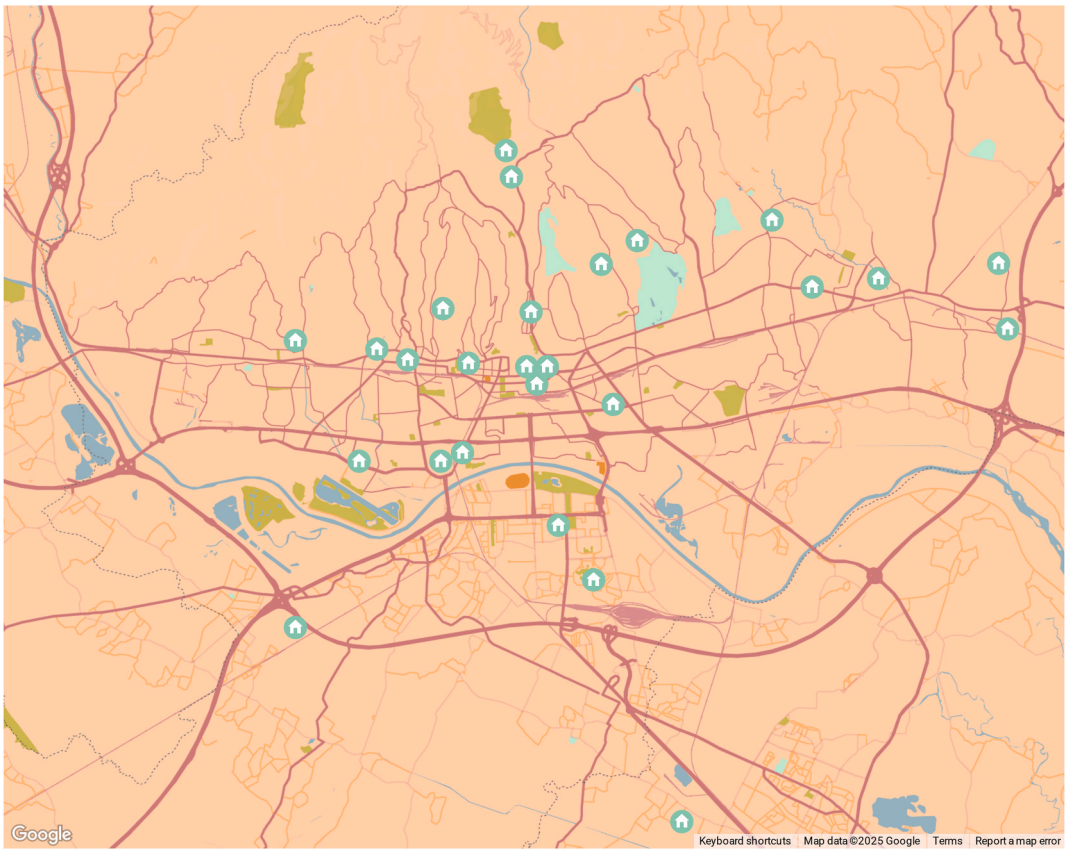

Fig. 1. Locations of indoor air sampling sites across 26 residential households in the City of Zagreb, Croatia. The selected households encompassed both high-traffic urban areas and suburban neighborhoods near green spaces, providing a representative assessment of indoor air pollution. Sampling was conducted from March to June 2023, covering both heating and non-heating periods to account for seasonal variability in exposure levels. Source: *Google Maps, accessed December 2025.*

processes. However, natural sources such as volcanic activity and wildfires are generally of limited significance when compared to human-driven emissions. Predominant anthropogenic contributors include incomplete combustion of organic matter during industrial operations, domestic heating, and road traffic (Choi H et al., 2010; Patel et al., 2020). Human exposure to PAHs occurs primarily via inhalation, though dietary intake of contaminated food and water, as well as dermal absorption, also represent meaningful pathways (Burchiel and Luster, 2001; Peng et al., 2011; Tong et al., 2018). Of particular concern is the indoor space, where PAHs tend to accumulate and often reach concentrations comparable to outdoor air, and in some cases can even exceed these levels during activities such as cooking or in poorly ventilated areas (Hartiala et al., 2025; Lovrić et al., 2024; Račić et al., 2025). Unlike outdoor air, which is subject to ambient air quality standards, indoor air lacks the regulatory oversight, except in specific occupational settings (Nassikas et al., 2024). Prolonged exposure to PAHs, especially in combination with other airborne toxicants, has been linked to a spectrum of chronic noncommunicable diseases as well as cancer (Hu et al., 2021; Kelly et al., 2021; Låg et al., 2020; Zhang et al., 2021). The severity of PAH-induced toxicity depends on several variables, including the route, duration, and dose of exposure, as well as individual factors such as age and pre-existing health conditions (Rajpara et al., 2017; Tong et al., 2018). Acute exposure to PAHs can result in symptoms such as eye irritation, respiratory discomfort (coughing, shortness of breath), gastrointestinal disorders, headache, dizziness or confusion, skin inflammation, and dermatitis (Abdel-Shafy and Mansour, 2016). Beyond these physiological effects, increasing evidence suggests that PM-bound PAHs exert toxic effects primarily through oxidative stress pathways and reactive oxygen species (ROS) production (Ewa and Danuta, 2017). Additionally, certain PAH metabolites, such as diolepoxides, pose heightened risks due to their low polarity, which hinders their excretion. These reactive intermediates covalently bind to DNA, forming stable adducts that disrupt genomic integrity and contribute to mutagenesis and genotoxicity (Abdel-Shafy and Mansour, 2016). Due to their physicochemical properties, PAHs exhibit high environmental persistence and mobility, allowing them to be widely distributed in air, water, and soil (Kim et al., 2013). Their ubiquitous presence has led to extensive investigation of their toxicological profiles. The International Agency for Research on Cancer (IARC) has reviewed the carcinogenic potential of 60 PAHs (IARC, 2010). Notably, benzo[a]pyrene is classified as a Group 1 human carcinogen. Other PAHs included in this study are categorized as Group 2A or 2B, indicating probable or possible carcinogenicity to humans, while some, such as benzo[ghi]perylene, fall under Group 3, reflecting inadequate evidence to determine their carcinogenic potential. The 11 PAHs investigated in this study were selected based on indoor air quality measurements conducted across residential households in the City of Zagreb (Croatia), and their respective IARC classifications are presented in Fig. 1 (IARC, 2010). Persistent accumulation of DNA damage resulting from exposure to PAHs and other environmental stressors compromises genomic stability, a central mechanism underlying the development of chronic noncommunicable diseases, including neurodegenerative and cardiovascular disorders, as well as cancer (Azqueta et al., 2020; Collins et al., 2014; Ladeira et al., 2024). Given that PAHs can exert toxic effects through multiple biological pathways, their cyto- and genotoxic potential cannot be adequately characterized using a single biological endpoint. Accordingly, genotoxic effects in the present study were evaluated using complementary assays targeting different levels of genome integrity: the alkaline comet assay, including

exploratory fractal and texture-based image analyses to capture subtle alterations in PAH-related DNA damage architecture, and the cytokinesis-block micronucleus (CBMN) assay to assess genome instability (Azqueta et al., 2020; Bonassi et al., 2016; Carpenter et al., 2006; Collins et al., 2023; Fenech, 2020; Fenech et al., 2020; Gajski et al., 2020, 2024; Gajski and Gerić, 2022; Ladeira et al., 2024; Møller, 2018; Schindelin et al., 2012; Schneider et al., 2012; Smith et al., 1989, 1996). When applied under controlled *in vitro* conditions, these assays enable sensitive detection of DNA and chromosomal damage across a range of exposure concentrations and durations. Despite extensive investigation of PAH toxicity, most experimental studies have focused on individual compounds or simplified mixtures, frequently tested at concentrations far exceeding those typically encountered in indoor environments. As a result, the relevance of such findings for real-scenario indoor exposure assessment remains limited. In contrast, the present study addresses this gap by translating measured residential indoor air PAH concentrations into defined short-term inhalation exposure scenarios, providing an experimental framework anchored to realistic indoor exposure conditions. The primary objective was to evaluate how environmentally relevant PAH concentrations influence cell viability and genomic stability across three human-derived biological models representing systemic and cell-specific responses. Within this framework, cells were exposed to a complex mixture of 11 PAHs formulated to reflect realistic indoor exposure scenarios corresponding to daily activity patterns. Given the importance of mixture toxicity in human health risk assessment, this approach enables a more accurate representation of cumulative PAH exposure compared with single-compound testing. In parallel, *in silico* toxicogenomic analysis was performed to identify shared molecular targets, disrupted signaling pathways, and potential gene-disease associations, thereby providing mechanistic insights into the toxicity of the complex PAH mixture. Together, this integrated experimental–computational approach advances current understanding of indoor PAH mixture toxicity beyond conventional single-compound or high-concentration models.

2. Materials and methods

2.1. Air pollution measurements

As part of the Horizon Europe project "Evidence Driven Indoor Air Quality Improvement" (EDIAQI, https://ediaqi.eu/) (Lovrić et al., 2025), the concentrations of PAHs associated with PM_1 (particles with an aerodynamic diameter $\leq$1 μm) were quantified in indoor environments. Indoor air sampling was carried out in 26 residential households distributed across the City of Zagreb (Croatia) to capture representative variability in indoor PAH levels. The sampling locations were strategically selected across diverse sites within the city, encompassing a range of microenvironments, including urban areas with high traffic density and suburban areas adjacent to green spaces, thereby capturing representative variations in exposure levels. This sampling strategy ensured a comprehensive assessment of indoor air pollution across the city, as shown in Fig. 1. Sampling took place from March to June 2023, capturing both heating and non-heating periods. PM_1 was collected using quartz fiber filters using an Air Metrics MiniVol™ sampler (Airmetrics, Eugene, USA) equipped with a size-selective impactor inlet for the PM_1 and a filter holder loaded with quartz filters (Whatman, Tisch Scientific, USA). The sampler operated at a constant flow rate of 5 L/min over a continuous 7-day sampling period. Quantification of PAHs bound to the PM_1 fraction was performed using high-performance liquid chromatography coupled with a fluorescence detector (HPLC/FLD; Agilent Technologies, USA). Detailed extraction and analytical protocols are available in Lovrić et al. (2024) and Jakovljević et al. (2018). In summary, the filters were extracted in an ultrasonic bath with a toluene–cyclohexane mixture (7:3), centrifuged, and evaporated to dryness under a nitrogen stream, after which the samples were re-dissolved in acetonitrile.

2.2. Preparation of the PAH mixture based on chemical analysis

The stock solution of the 11-PAH mixture was prepared from certified reference standards of individual PAHs (Supelco, Sigma Aldrich, Merck, Germany). Fluoranthene (Flu), benzo[b]fluoranthene (BbF), dibenzo[ah]anthracene (DahA), and benzo[ghi]perylene (BghiP) were used at concentrations of 200 μg/mL, while pyrene (Pyr), benzo[a]anthracene (BaA), chrysene (Chry), benzo[k]fluoranthene (BkF), benzo[a]pyrene (BaP), and indeno[1,2,3-cd]pyrene (IP) were used at 100 μg/mL reflecting the concentrations measured across the sampled households. An appropriate volume of each individual PAH standard solution was added to a vial, and the resulting mixture was evaporated to complete dryness under a stream of nitrogen. The dried residues were then re-dissolved in dimethyl sulfoxide (DMSO). From this stock solution, three diluted stock solutions in DMSO were prepared to represent three exposure scenarios: low (1-h exposure), medium (8-h exposure), and high (16-h exposure). The low and medium exposure concentrations corresponded to normal activity, while the high exposure concentration represented a combination of resting and normal activity conditions. Exposure periods were calculated based on minute ventilation values (L/min), derived from tidal volume (L/breath) and respiratory rate (breaths/min) under rest and normal activity conditions (Pleil et al., 2021). These calculations provided estimates of the total volume of air exchanged by the lungs during inhalation and exhalation over 1-, 8-, and 16-h intervals, with minute-to-hour conversions applied (Table 1). This approach yielded total inhaled volumes of 960 L for the low (1-h normal activity), 7680 L for the medium (8-h normal activity), and 10,560 L for the high exposure scenario, the latter accounting for 8 h at rest and 8 h of normal activity. Since PAH concentrations are expressed in nanograms per cubic meter (ng/m^3), the volumes were converted from cubic meters to liters, and subsequently to milliliters, to enable accurate preparation of the stock solutions (see Supplementary Table 1).

2.3. Toxicological characterization

2.3.1. Cell models

Whole blood was obtained from three healthy, non-smoking adult volunteers (two females, one male; aged 27–31 years) residing in Zagreb (Croatia). Donors had no recent exposure to ionizing radiation or known genotoxic chemicals and were instructed to avoid exposure to passive smoking in enclosed spaces within 24 h prior to sample collection. Venous blood was collected in the morning into coded heparinized tubes (Becton Dickinson, USA) by a certified technician, kept at 4 °C, and processed within 1 h. Whole blood was then exposed to low, medium, or high concentrations of the 11-PAH mixture (Supplementary Table 1) for 4 and 24 h. For specific assays, different blood cell subpopulations were used: peripheral blood cells (PBCs) were used for the comet assay, peripheral blood mononuclear cells (PBMCs) isolated by density gradient centrifugation were used for differential staining cytotoxicity assessment, and human peripheral blood lymphocytes (HPBLs) were used for the cytokinesis-block micronucleus (CBMN) assay. For simplicity and consistency throughout the manuscript, these blood-derived cell populations are collectively referred to as PBCs, unless otherwise specified. Informed consent was obtained from all participants, and the study was approved by the Ethics Committee of the Institute for Medical Research and Occupational Health, in accordance with the Declaration of Helsinki. To complement the whole-blood experiments, *in vitro* studies were conducted using A549 (human alveolar epithelial; ATCC-CCL-185™, Manassas, USA) and HepG2 (human hepatocellular carcinoma; ATCC-HB-8065™, Manassas, USA) cell lines obtained from the American Type Culture Collection (ATCC, USA). The cells were cultured at 37 °C in a humidified atmosphere containing 5% CO_2. A549 cells were maintained in low-glucose Dulbecco's Modified Eagle's Medium (DMEM; D6046, Sigma-Aldrich, Germany) supplemented with 10% (*v/v*) fetal bovine serum (FBS; Gibco, Thermo Fisher Scientific), 1% penicillin–streptomycin (100 U/mL and 100 μg/mL; Sigma-Aldrich), and 2

Table 1
Breathing parameters and exposure scenarios for healthy adults. The table summarizes the exposure scenarios based on breathing parameters calculated for healthy adults. Low concentration corresponds to a 1-h exposure during normal activity, medium concentration represents an 8-h exposure during normal activity, and high concentration accounts for a 16-h exposure combining 8 h of rest and 8 h of normal activity.

Condition	Respiratory Rate (breaths/min)	Tidal Volume (L/breath)	Minute Ventilation (L/min)	1 h (L)	8 h (L)	16 Hours (L)
At Rest	12	0.5	6	360	2880	5760
Normal Activity	16	1	16	960	7680	15360

mM L-glutamine (Sigma-Aldrich). HepG2 cells were grown in Minimum Essential Medium (MEM; Gibco, Thermo Fisher Scientific, UK) supplemented with 10% FBS (Gibco), 1 mM sodium pyruvate, 2 mM L-glutamine, and 100 IU/mL penicillin–streptomycin (Sigma-Aldrich, USA). Cells were used between 3 and 10 passages once they reached approximately 80–90% (A549) or 70% (HepG2) confluency, seeded at appropriate densities, and treated with the 11-PAHs mixture for 4 or 24 h as indicated.

2.3.2. Cell viability (cytotoxicity) assays

Cell viability was assessed using fluorescence-based and colorimetric assays following established protocols by Atale et al. (2014) for PBMCs which were isolated from whole blood as mentioned in Section 2.3.1., Alley et al. (1988) for A549, and Mosmann (1983), with minor modifications (Novak et al., 2016) for HepG2 cells. Different cytotoxicity assays were selected based on methodological suitability for each cell model. Membrane integrity-based assessment was applied to the primary, non-adherent cell population of PBMCs, whereas a metabolic activity-based assay was used for adherent A549 and HepG2 cells. Accordingly, cytotoxicity results were interpreted within each cell model, and direct quantitative comparisons between blood-derived and immortalized cell lines were avoided. For PBMCs, viability was evaluated by acridine orange/ethidium bromide (AO/EtBr) differential staining. After treatment of whole blood, PBMCs were isolated by Histopaque-1077 density gradient centrifugation (Sigma-Aldrich), and 200 μL of PBMC suspension was mixed with 2 μL of AO/EtBr, both diluted in PBS. A total of 100 cells per repetition (four technical replicates) were analyzed using an epifluorescence microscope (Olympus BX51, Japan). Cells with uniform green nuclear staining were classified as viable, while red-stained nuclei indicated nonviable cells. A solvent control (0.1% DMSO) was included. For A549 and HepG2 cells, cytotoxicity was determined by the MTT [3-(4,5-dimethylthiazol-2-yl)-2, 5-diphenyltetrazolium bromide] reduction assay. Cells were seeded in 96-well plates and allowed to attach before exposure to PAH mixtures. After treatment, MTT solution (5 mg/mL stock, diluted in medium) was added and incubated to allow for formazan formation, which was then solubilized with DMSO, and absorbance was read using a microplate reader (SpectraMax iD3, Molecular Devices, USA, or Synergy MX, BioTek, USA). Specific conditions were as follows: A549, 5×10^4 cells/mL, 4-h MTT incubation, absorbance at 545 nm; HepG2, 40000 cells/mL, 3-h MTT incubation, absorbance at 570 nm with 690 nm reference. A minimum of four (A549) or five (HepG2) technical replicates across three independent experiments were analyzed. Negative (fresh medium), solvent (0.1% DMSO), and positive (0.5 μM etoposide for A549 and 4% DMSO for HepG2) controls were included in each experiment.

2.3.3. DNA damage

2.3.3.1. Comet assay. The alkaline comet assay was performed according to Collins et al. (2023) and Minimum Information for Reporting Comet Assay (MIRCA) guidelines (Møller et al., 2020), with minor modifications for human PBCs (Gajski et al., 2016) using whole peripheral blood as described in Section 2.3.1., A549 (Jugan et al., 2012), and HepG2 (Novak et al., 2017) cell lines. Whole blood (5 μL) or cell suspensions (20 μL for A549 and 30 μL for HepG2) were mixed with low-melting-point (LMP) agarose (Merck) and layered onto slides pre-coated with normal-melting-point (NMP) agarose (Merck): 0.5% LMP/0.6% NMP for PBCs, 0.5%/0.5% for A549, and 1%/1% for HepG2. After solidification, for PBCs and A549 cells, slides were overlaid with a second LMP layer and lysed at 4 °C in solution containing 2.5 M NaCl, 100 mM EDTA-Na_2, 10 mM Tris-HCl, 1% Triton X-100 (Merck), and 10% DMSO (Kemika, Croatia), pH 10. For HepG2 cells, slides were lysed without an additional LMP layer and without DMSO under otherwise identical conditions. DNA was then unwound and electrophoresed in alkaline solution [300 mM NaOH (Kemika), 1 mM EDTA-Na_2 (Merck), pH $>$ 13] at 4 °C, followed by neutralization (0.4 M Tris, pH 7.5). Staining and analysis were performed as follows: PBCs were stained with EtBr (10 μg/mL) and analyzed by epifluorescence microscopy (Zeiss, Germany) using Comet Assay II (Perceptive Instruments Ltd., UK); A549 slides were stained with EtBr (20 μg/mL) and examined under an Olympus BX51 microscope (Japan) with Comet Assay IV; HepG2 slides were stained with GelRed (Biotium, USA) and analyzed on a Nikon Eclipse 800 microscope (Japan) using Comet Assay IV. In all cases, a minimum of 150 nuclei per experimental point was scored. Minor protocol variations included overnight lysis and electrophoresis at 1 V/cm for 20 min in PBCs, shorter lysis ($\geq$1 h) and 0.7 V/cm for 24 min in A549, and shorter lysis ($\geq$1 h) and 1 V/cm for 20 min in HepG2. Negative (fresh medium), solvent (0.1% DMSO), and positive [1 mM H_2O_2 (Kemika) for PBCs, 5 μM etoposide (Santa Cruz Biotechnology, USA) for A549, and 30 μM BaP (Merck) for HepG2] controls were included in each experiment.

2.3.3.2. Image-based morphometric and multifractal analysis. Comet assay images derived from measurements in PBCs were analyzed in ImageJ (NIH) using the FracLac plugin and custom Mathematica scripts to extract morphometric descriptors (see Supplementary Material). Fractal and multifractal spectra were computed by the box-counting method across $Q = -10$ to 10 (step 0.1), yielding generalized dimensions DQ and singularity spectra f(α). Shape parameters (Area, Perimeter, Circularity, Eccentricity) and gray-level co-occurrence matrix (GLCM) features (Entropy, ASM, IDM, Contrast) were derived for each image. Data were aggregated per treatment (low, medium, high) and time point (4 and 24 h). This exploratory analysis complemented standard comet endpoints and was not used for statistical decision-making. As an exploratory approach, comet images were also represented using a graph-based framework, where comet pixels or defined components are treated as connected nodes (Godrèche et al., 1992; Lund et al., 2009). This allows the use of simple topological descriptors and concepts from persistent homology to examine overall organization and structure within the comet image.

2.3.4. Genomic instability

The CBMN assay was conducted according to Fenech (2007), with minor modifications for human peripheral blood lymphocytes (HPBLs) (Gajski et al., 2026), A549 (Jakšić et al., 2012), and HepG2 (Novak et al., 2017). After treatment, cultures were incubated at 37 °C in a humidified 5% CO_2 atmosphere, and cytokinesis was arrested with cytochalasin B (Merck) at the indicated concentrations to enable binucleated cell formation. For HPBLs, 500 μL of whole blood was cultured in Chromosome KIT P medium (Euroclone S.p.A., Italy), which contains phytohemagglutinin (PHA), a mitogen that selectively stimulates lymphocytes to enter the cell cycle, thereby enabling their proliferation and subsequent

analysis in the CBMN assay (Gajski et al., 2026). Cytochalasin B (6 μg/mL) was added 44 h post-culture initiation, and cells were harvested after 72 h, fixed in methanol:acetic acid (3:1, *v/v*; Kemika), and air-dried. Slides were stained with 3% Giemsa (Merck) and scored microscopically (Zeiss Axiolab 5, Germany). For A549 cells, cytochalasin B (3 μg/mL) was added concurrently with or immediately after exposure to the 11-PAH mixture as described by Fernández-Bertólez et al. (2021). Cells grown on glass coverslips (Falcon, USA) were initially fixed using a methanol–glacial acetic acid solution (5:1, *v/v*) diluted with an equal volume of distilled water, followed by three additional fixation steps with undiluted methanol–glacial acetic acid (5:1, *v/v*), and then stained with 7% Giemsa before microscopic scoring (Zeiss Axiolab 5). For HepG2, cells were seeded in 6-well plates and allowed to adhere for 24 h before exposure to the 11-PAH mixture for 24 h. After treatment, cells were washed with PBS and incubated for an additional 26 h in fresh medium containing cytochalasin B (2 μg/mL). Cells were then fixed in methanol:acetic acid (3:1, *v/v*) and formaldehyde, air-dried, stained with DAPI Vectashield (Vector Laboratories, USA), and analyzed using the Metafer automated imaging system (MetaSystems, Germany).

Micronuclei (MNi), nuclear buds (NBUDs), and nucleoplasmic bridges (NPBs) were scored in at least 1000 binucleated cells per experimental point, following the criteria of Fenech et al. (2020). Each assay included negative (fresh medium), solvent (0.1% DMSO), and positive (10 μg/mL bleomycin for HPBLs, 0.3 μg/mL etoposide for A549, and 0.1 μg/mL etoposide for HepG2) controls. The cytokinesis-block proliferation index (CBPI) was calculated across all cell types based on 500 cells per condition using the formula: $CBPI = [M1 + 2M2 + 3(M3 + M4)]/500$, where M1–M4 represent the number of cells with one to four nuclei, respectively (Gajski et al., 2026).

2.4. In silico toxicogenomic data analysis

An *in silico* toxicogenomic assessment was carried out using publicly accessible databases, software platforms, and computational tools, in order to provide a mechanistic context for the experimental findings and to determine whether the PAHs detected in indoor air converge on shared molecular pathways that could explain the observed biological responses. The analysis was performed using the Comparative Toxicogenomics Database (CTD) (http://ctdbase.org; North Carolina State University, USA). This database was used to identify gene/protein biomarkers and explore how multiple chemicals simultaneously influence gene expression and protein activity, an approach highly relevant for evaluating mixture toxicity and extracting relevant gene/protein biomarkers (Baralić et al., 2022; Davis et al., 2019; Mattingly et al., 2006). The database is regularly updated to ensure the accuracy, consistency, and usability of its content (Davis et al., 2019). GeneMANIA (https://genemania.org) was used to characterize the relationships within the obtained gene set. The platform incorporates proteomic and genomic datasets to identify genes with similar functions and to map several types of interactions (Warde-Farley et al., 2010), including co-expression, which indicates similar expression patterns; predicted interactions, typically involving inferred protein–protein interactions; shared biological pathways; direct physical interactions between proteins; common protein domains; co-localization within the same tissue, compartment, or protein complex; and genetic interactions, in which altering one gene influences the effect of another. The ToppGene Suite (https://toppgene.cchmc.org), particularly its ToppFun tool, was employed for functional enrichment analysis. This tool examines gene ontology categories (biological processes, molecular functions, cellular components), molecular pathways, disease associations, and other functional attributes, which can help explore toxicity mechanisms (Chen et al., 2009).

The investigated PAHs were analyzed through several steps: extracting Gene–PAH interaction data from CTD; identifying shared genes using the CTD MyVenn tool (excluding PAHs with fewer than five associated genes from defining the common set, though they were included later in the cumulative analysis); assessing gene–gene interactions with GeneMANIA; and performing functional enrichment with ToppGene Suite to identify key molecular functions, biological processes, pathways, and disease associations. After defining the common gene set, all genes interacting with the PAHs were compiled into a cumulative set with duplicates removed. Evaluating both the shared and cumulative genes enabled identification of common toxicity mechanisms, potentially reflecting additive or synergistic effects, as well as additional PAH-specific pathways relevant to their broader molecular impact. GeneMania network analysis could not be performed for this full set due to the GeneMANIA 3000-gene input limit.

2.5. Statistical analysis

All statistical analyses were performed using R software (version 4.4.3; R Core Team, Austria). Data were tested for normality and homogeneity of variance prior to analysis. Cell viability (cytotoxicity) and comet assay (log-transformed tail intensity) data were analyzed using one-way analysis of variance (ANOVA), followed by Tukey's honest significant difference (HSD) post hoc test to assess pairwise differences between treatments and controls. Genomic instability endpoints obtained from the CBMN assay, namely, MNi, NBUDs, NPBs, and CBPI, were analyzed as count data with a quasi-Poisson distribution. As the data did not conform to parametric assumptions, a non-parametric Kruskal–Wallis test was used, followed by Dunnett-type post hoc comparisons to assess differences between treatment groups and the solvent control. To account for multiple testing and reduce the risk of Type I errors, p-values were adjusted using the Holm–Bonferroni correction method across all post hoc analyses. Statistical significance was considered at $p < 0.05$. All data are presented as mean ± standard deviation (SD), unless otherwise specified. Graphs and visualizations were generated using the ggplot2 package (Wickham, 2016).

3. Results

3.1. Indoor air quality and PAH detection

Analysis of PM_1 samples collected from indoor environments (N = 26) identified and quantified 11 target PAHs: BaP, BghiP, DahA, Chry, BkF, BbF, BjF, Flu, Pyr, and IP. Concentrations of these compounds, expressed as median values (ng/m^3), along with corresponding means and ranges (minimum–maximum), are summarized in Table 2. The identified PAHs were further classified according to their

Table 2
Concentrations of 11 PAH compounds measured in indoor air. Concentrations of PAHs detected are expressed as median, mean and range (minimum and maximum) values measured in households across the City of Zagreb (N = 26) sampled between March and June 2023.

PAH	Median [ng/m^3]	Mean [ng/m^3]	Minimum [ng/m^3]	Maximum [ng/m^3]
Flu	0.109	0.115	0.007	0.325
Pyr	0.086	0.099	0.010	0.286
BaA	0.024	0.043	ND	0.295
Chry	0.063	0.110	0.002	0.912
BjF	0.101	0.221	0.005	2.185
BbF	0.160	0.248	0.007	2.025
BkF	0.044	0.081	0.001	0.731
BaP	0.104	0.148	0.002	0.993
DahA	0.015	0.030	ND	0.179
BghiP	0.174	0.226	0.002	1.524
IP	0.177	0.260	0.006	2.078

Benzo[a]anthracene (BaA), benzo[a]pyrene (BaP), benzo[b]fluoranthene (BbF), benzo[ghi]perylene (BghiP), benzo[j]fluoranthene (BjF), benzo[k]fluoranthene (BkF), chrysene (Chry), dibenzo[a,h]anthracene (DahA), fluoranthene (Flu), indeno[1,2,3-cd]pyrene (IP), pyrene (Pyr), non-detectable (ND).

carcinogenicity based on IARC classifications, as shown in Fig. 2. Their relative contributions to total indoor PAH content are presented in Fig. 3, with percentage values derived from the same median concentrations reported in Table 2. To contextualize experimental exposures, modelled breathing scenarios based on physiological parameters for healthy adults were used to estimate realistic indoor PAH exposures. These scenarios are presented in Table 1, with low exposure corresponding to a 1-h exposure during normal activity, medium exposure representing 8 h of normal activity, and high exposure reflecting a 16-h period consisting of 8 h of rest followed by 8 h of normal activity.

3.2. Cytotoxicity

Cell viability was evaluated across all three cell types following exposure to 11 PAHs mixture under different exposure durations, as shown in Fig. 4A. For blood-derived models, cytotoxicity was specifically assessed in PBMCs, which were isolated from whole blood prior to analysis. It is important to note that cytotoxicity in PBMCs was assessed using AO/EtBr differential staining, which morphologically distinguishes live from dead cells based on membrane integrity, whereas cytotoxicity in A549 and HepG2 cells was evaluated using the MTT assay, which relies on mitochondrial succinate dehydrogenase activity as an indicator of cell viability. As a result, only the cytotoxic responses of A549 and HepG2 cells were directly comparable. In PBMCs, a clear concentration- and time-dependent decrease in cell viability was observed across all exposure scenarios. The most pronounced cytotoxic effects were seen following 24-h treatments, with the lowest cell viability measured at the highest PAH concentration corresponding to the 16-h exposure period (high). In A549 cells, a reduction in cell viability was observed following 4-h exposures in all scenarios, although these decreases were not statistically significant. Similarly, HepG2 cells showed a slight, non-significant decrease in viability after 24 h of treatment, suggesting a relatively lower sensitivity to the tested PAHs at the applied concentrations. No statistically significant differences in proliferation kinetics were observed across any of the cell lines, as measured by the CBMN assay CBPI (Fig. 4B).

3.3. Induction of DNA damage

DNA strand breakage was evaluated across all three cell types using the tail intensity (TI) descriptor of the alkaline comet assay after different exposure durations. To enable comparison between cell models, DNA damage results are expressed as the relative increase in TI compared to corresponding vehicle controls, as shown in Fig. 5. Across all cell types, PAH-induced DNA damage was not statistically significantly different compared to vehicle controls; however, a subtle increase in TI after 24-h treatment was observed in PBCs at low and medium PAH concentrations (23% and 49% relative increase compared to control), corresponding to the 1- and 8-h exposure scenarios, respectively. In A549 cells, a modest, non-concentration-dependent increase in TI was

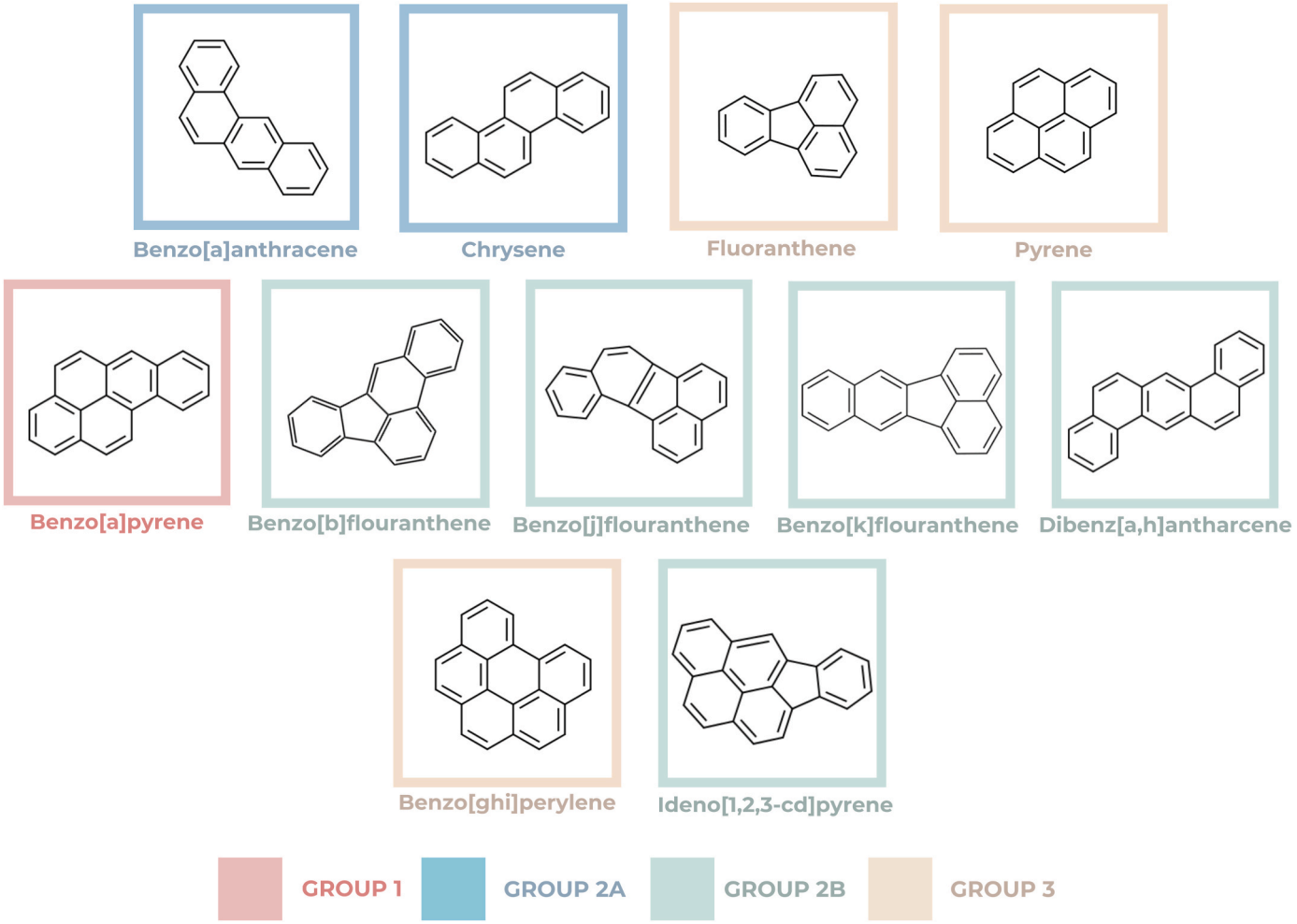

Fig. 2. Chemical structures and IARC classifications of 11 PAHs detected in indoor PM_1. The figure illustrates the molecular structures of the 11 detected PAHs, each categorized according to the IARC classification system: Group 1 (carcinogenic to humans, red), Group 2A (probably carcinogenic to humans, blue), Group 2B (possibly carcinogenic to humans, green), and Group 3 (not classifiable as to its carcinogenicity to humans, beige).

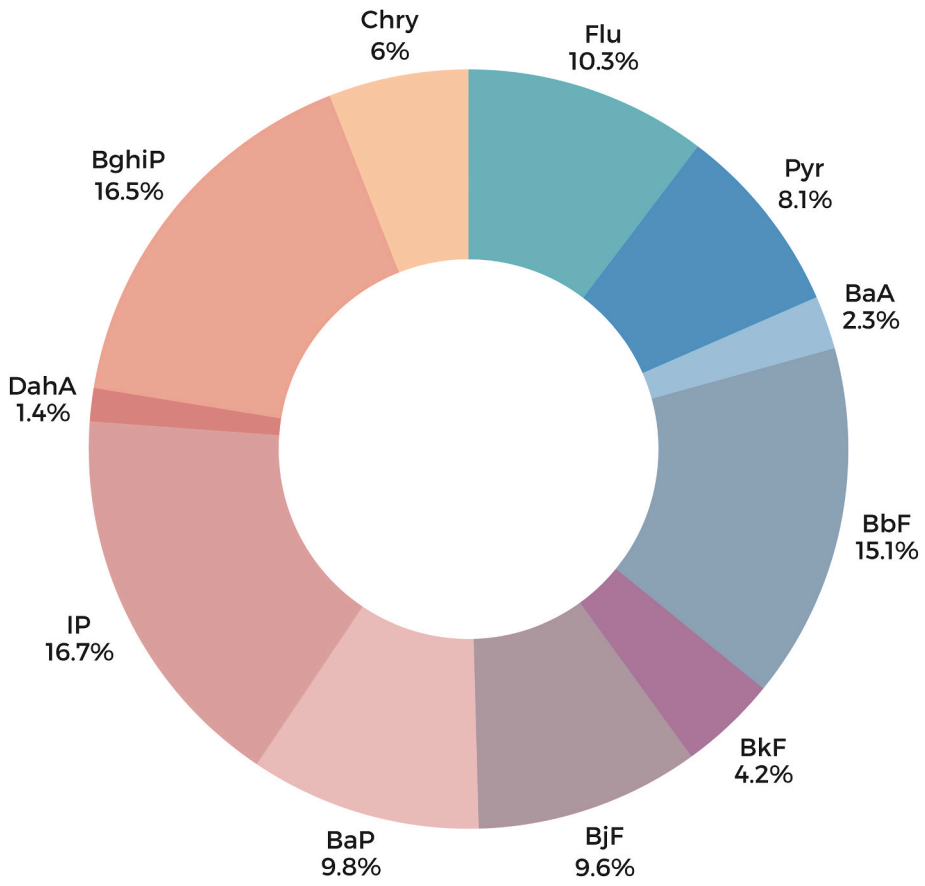

Fig. 3. Relative contribution of detected PAHs in indoor PM_1 samples. Ring chart representing the proportional contribution (%) of each of the 11 targeted PAHs measured in the PM_1 fraction of indoor air. The percentages are based on median concentration values reported in Table 2. The most abundant compounds were IP (16.7%), BghiP (16.5%), and BbF (15.1%), collectively accounting for nearly half of the total PAH load. The lowest proportions were observed for DahA (1.4%) and BaA (2.3%). Benzo[a]anthracene (BaA), benzo[a]pyrene (BaP), benzo[b]fluoranthene (BbF), benzo[ghi]perylene (BghiP), benzo[j]fluoranthene (BjF), benzo[k]fluoranthene (BkF), chrysene (Chry), dibenzo[a,h]anthracene (DahA), fluoranthene (Flu), indeno[1,2,3-cd]pyrene (IP), pyrene (Pyr).

observed following 24-h exposure (up to 33% relative increase compared to control), whereas HepG2 cells exhibited no significant changes. HepG2 cells exhibited no significant increase in DNA damage following 24-h exposure, with TI values comparable to vehicle control groups. Positive controls induced a clear and statistically significant response, confirming the sensitivity and reliability of the assay. Exploratory morphometric analysis was performed exclusively in PBCs, as this was the only cell model that exhibited a positive genotoxic response to PAH exposure, enabling a more sensitive assessment of potential image-based correlates of DNA damage; however, no statistically significant correlations between morphometric parameters and PAH concentrations were observed. In PBCs comet images, compared with 4-h exposure, 24-h images exhibited higher morphological uniformity, whereas 4-h images showed broader multifractal spectra and greater local heterogeneity. Haralick features Entropy and ASM: Angular Second Moment (Homogeneity) are related to the exposure level at 4 h. Generalized dimensions DQ decreased stepwise with exposure, indicating a subtle simplification of comet architecture (see Supplementary Material). These findings align with the modest increases the modest increases in TI, suggesting nuanced alterations in DNA damage morphology rather than magnitude.

3.4. Induction of genomic instability

The induction of genomic instability by the 11-PAH mixture was further assessed using the CBMN assay. In addition to the evaluation of MNi (Fig. 6A), the formation of NBUDs (Fig. 6B) and NPBs (Fig. 6C) were also quantified. To facilitate comparison across models, the results are expressed as the relative increase in assay parameters frequency compared to background levels in vehicle control (control = 1, without SD) cells. For blood-derived samples, genomic instability was specifically assessed in HPBLs, which were selectively stimulated to proliferate for CBMN analysis and are considered a defined subpopulation of PBCs. In HPBLs, a concentration-dependent increase in MNi frequency was observed following both 4-h (up to 3.20-fold) and 24-h (up to 2.58-fold) exposures, although these increases were not statistically significant. Notably, HPBLs also showed an increase in both NBUDs and NPBs, with a statistically significant increase of NPBs observed at the medium PAH concentration following 24-h treatment (frequency increased from 0 in control cells to 3.67 per 1000 binucleated cells). In A549 cells, a slight increase in MNi frequency was detected at the medium 11 PAH mixture concentration (53% relative increase compared to control) after 4-h treatment, while no notable changes were observed after 24 h. HepG2 cells exhibited no significant increase in MNi frequency at any concentration or exposure scenario following 24-h treatment, aligning with the absence of DNA damage observed in the comet assay.

3.5. Results of in silico toxicogenomic data analysis

All extracted genes associated with the analyzed PAHs can be seen in Supplementary Table 2. The number of gene interactions varied markedly across compounds, with the highest observed for BaP (19,890 interactions), followed by BbF (1,685), BaA (1,414), Chry (962), Flu (957), DahA (915), BkF (754), Pyr (303), BghiP (306), IP (261), and the lowest in BjF (5). The four genes *AHR, CYP1A1, CYP1B1*, and *NQO1* were common to all PAHs present in the tested mixture when BjF was

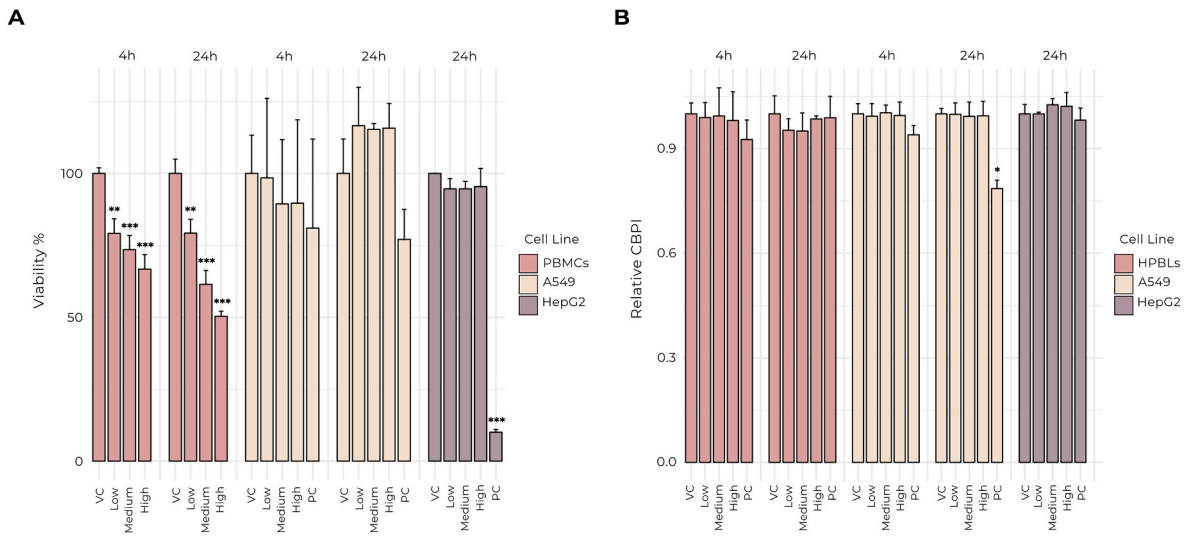

Fig. 4. Viability responses in human peripheral blood mononuclear cells (PBMCs) and proliferation kinetics in human peripheral blood lymphocytes (HPBLs) following exposure to an indoor air-derived 11-PAH mixture, with comparative effects in lung epithelial cells (A549), and hepatocellular carcinoma cells (HepG2). PBMCs and HPBLs represent distinct peripheral blood cell subpopulations used for cytotoxicity and proliferation analyses, respectively. (**A**) Cell viability following exposure to low (1-h exposure scenario), medium (8-h exposure scenario), and high (16-h exposure scenario) concentrations of a PAHs mixture, derived from indoor air measurements across 26 households in Zagreb (Croatia). Viability was assessed using AO/EtBr differential staining in human PBMCs and the MTT assay in A549 and HepG2 cells. Vehicle control (VC): 0.1% DMSO. Positive controls (PC): 0.5 μM etoposide (A549), 4% DMSO (HepG2). Data are normalized to 100% viability and presented as mean +standard deviation (SD). $^{**}p < 0.01$, $^{***}p < 0.001$. (**B**) Cytokinesis-block proliferation index (CBPI) values calculated from 500 cells with one to four nuclei following the same PAH exposure scenarios, used to evaluate proliferation kinetics and potential cytostatic effects. PC: bleomycin (10 μg/mL, HPBLs), 0.3 μg/mL etoposide (A549), and 0.1 μg/mL etoposide (HepG2). VC was 0.1% DMSO for all cell types. Data shown as mean +SD. $^{*}p < 0.05$.

excluded from the analysis. When BjF was included, the genes shared across all PAHs were *AHR, CYP1A1*, and *CYP1B1*. Although *NQO1* was not shared by BjF, it was retained in the common gene set due to its consistent presence across all other PAHs, highlighting its relevance to the overall PAH response pattern. These four common genes (*AHR, CYP1A1, CYP1B1*, and *NQO1*) were involved mainly in physical interactions (Fig. 7). Co-expression represented the second most frequent type of connection, while predicted interactions accounted for a smaller but relevant proportion of the total functional links. Functional analysis of the four common genes (*AHR*, *CYP1A1*, *CYP1B1*, *NQO1*) identified the most significant molecular functions, biological processes, cellular components, molecular pathways, and associated diseases (Table 3).

When all genes interacting with the examined PAHs are considered (the cumulative gene set), a total of 20,403 genes is obtained. As presented in Table 4, functional analysis of this gene set highlights the most significant molecular functions, biological processes, cellular components, pathways, and associated diseases.

4. Discussion

In this study, we assessed the cytogenotoxic responses of human blood cells, along with human-derived liver (HepG2) and lung (A549) cell lines, to a defined mixture of 11 PAHs commonly detected in indoor air across households in Zagreb (Croatia). These cell models were selected to capture both systemic and cell-specific responses, representing key biological targets involved in human exposure to airborne pollutants. While human health risk assessments are typically based on toxicity data from individual compounds, our approach emphasizes the relevance of toxicological assessment of complex, environmentally relevant mixtures (Bopp et al., 2018, 2019; Hayes et al., 2019; Rotter et al., 2018). This is particularly important considering the known carcinogenic potential of certain PAHs and the fact that humans are exposed daily to complex mixtures rather than single compounds, using exposure concentrations that reflect real-life indoor conditions, as determined from household indoor air quality measurements. By simulating realistic 1-, 8-, and 16-h exposure scenarios, our study provides a closer approximation of potential human health risks associated with environmentally relevant indoor PAHs exposure.

4.1. Cytotoxicity

The cytotoxicity results, as measured by the AO/EtBr assay for human PBMCs and the MTT assay for A549 and HepG2 cells, revealed distinct differences across the cell types (Fig. 4A). PBMCs were the most sensitive to PAH-induced cytotoxicity, with cell viability declining to approximately 50% at the highest concentration (16-h exposure scenario) following 24-h exposure. Statistically significant time- and concentration-dependent reductions in viability were observed, likely reflecting their untransformed status and limited detoxification and repair capacity compared to immortalized lines, making them more vulnerable to PAH-induced oxidative stress and cell death (Ewa and Danuta, 2017; Li et al., 2024; Marino et al., 2024). In contrast, A549 cells, being tumor-derived and highly proliferative, did not show significant cytotoxicity after PAH exposure under our experimental conditions. Notably, A549 cells express metabolic enzymes such as cytochrome P450 1A1 (CYP1A1) that can activate certain xenobiotics and support genotoxic responses without necessarily triggering acute cytotoxicity (Carero et al., 2001; Foster et al., 1998; Gminski et al., 2010). Furthermore, Takam et al. (2024) found that A549 cells exposed to 0–400 μM phenanthrene, Flu, or BghiP for 24 h exhibited decreased viability only at higher PAH concentrations, while lower, environmentally relevant concentrations induced genotoxic effects (increased MNi) without prominent cytotoxicity. In our study, A549 cells showed a slight reduction in viability at 4 h, whereas 24-h exposure led to increased viability relative to controls, suggesting a potential hormetic effect, where low-dose PAHs may stimulate metabolic activity and proliferation in transformed cells (Calabrese and Mattson, 2017). HepG2 cells showed a negligible cytotoxic response across all tested PAH concentrations, consistent with previous reports from Dong et al. (2020), showing minimal impact at 10–50 μg/mL and only slight reductions at 100 μg/mL sediment-derived PAH mixture. In the study by Dong et al. (2020), HepG2 cells were notably more tolerant to PAH exposure than

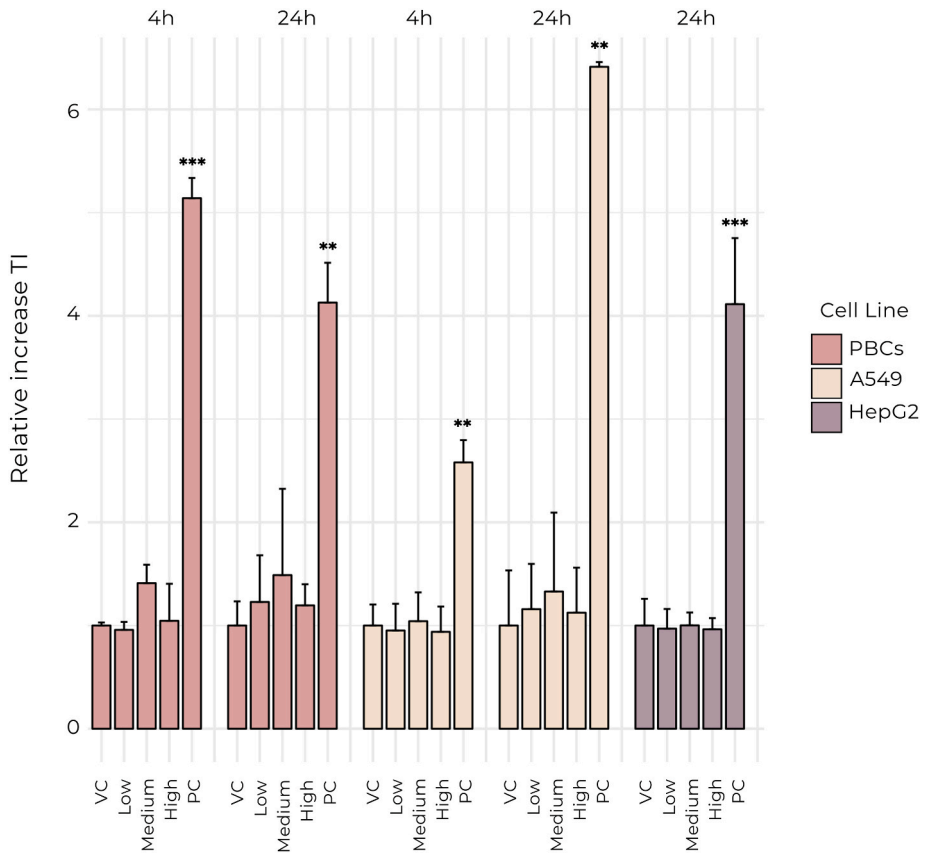

Fig. 5. Induction of DNA strand breaks in human peripheral blood cells (PBCs), lung epithelial cells (A549), and hepatocellular carcinoma cells (HepG2) following exposure to an indoor air-derived 11-PAH mixture at varying concentrations and durations. DNA strand breakage was evaluated using the alkaline comet assay and expressed as Tail Intensity (TI), calculated for at least 150 comets per experimental point. Cells were exposed to low (1-h exposure), medium (8-h exposure), and high (16-h exposure) concentrations of a PAH mixture derived from indoor air monitoring in Zagreb (Croatia) households. Positive controls (PC): hydrogen peroxide (1 mM, PBCs), 5 μM etoposide (A549), and 30 μM benzo[a]pyrene (HepG2). Vehicle control (VC; 0.1% DMSO) was used for all cell types. TI data were log-transformed prior to analysis. Statistical comparisons between VC and treatments were performed using one-way analysis of variance (ANOVA), followed by Tukey's honest significant difference (HSD) post hoc test. Holm–Bonferroni correction method was used to adjust the p-values. Data are presented as mean values +standard deviation (SD) of the relative increase in TI over VC levels. **$p < 0.01$, ***$p < 0.001$.

the zebrafish (*Danio rerio*) embryonic cell line (ZF4), which exhibited marked cytotoxicity at similar or lower concentrations. Studies with immortalized bronchial epithelial cells (BEAS-2B) revealed comparable cytotoxicity profiles to HepG2, reinforcing the notion that immortalized cell lines are relatively resistant to PAH-induced cytotoxicity (Jiang et al., 2023). Notably, Takam et al. (2024) highlighted that the concentrations of PAHs inducing cytotoxicity in A549 co-culture with macrophages (THP–1) were much higher than those that produced genotoxicity, further supporting that the PAH concentrations used in our study, which reflect real-life indoor air exposures, are likely to reveal differential sensitivity between primary and immortalized cell models. Despite statistically significant, time- and concentration-dependent cytotoxicity in PBMCs, no notable impact on cellular proliferation kinetics was observed following exposure, as presented by CBPI across all cell types (Fig. 4B). These early cytotoxic responses in PBMCs did not translate into prolonged inhibition of cell proliferation, indicating that the surviving cell population retained normal proliferative capacity. The greater sensitivity observed in primary blood-derived cells compared with A549 and HepG2 cells likely reflects differences in metabolic capacity and genome stability. Human PBCs are normal primary cells with a stable genome and limited metabolic activity, particularly with respect to phase I and phase II xenobiotic-metabolizing enzymes (Gajski et al., 2018; Gajski and Gerić, 2022), which may reduce their ability to detoxify PAHs or reactive intermediates and increase susceptibility to cytotoxic effects at low exposure levels. In contrast, HepG2 cells retain functional phase I and phase II metabolic enzymes involved in xenobiotic biotransformation (Madunić et al., 2022), which may contribute to greater tolerance toward low-dose PAH exposure. These biological differences provide a mechanistic basis for the preferential cytotoxic sensitivity observed in blood-derived cells, while transformed epithelial and hepatic cell lines exhibited muted responses under the same environmentally relevant exposure conditions.

4.2. Genotoxicity

In our study, DNA damage was assessed using the comet assay (TI) and chromosomal instability using the CBMN assay (MNi, NBUDs, NPBs) in PBCs, A549, and HepG2 cells exposed to environmentally relevant indoor PAH mixtures. Across all cell lines and exposure durations (4 and 24 h), no statistically significant increase in DNA strand breaks was observed, with TI fold changes remaining close to one (Fig. 5). In PBCs, both 4-h and 24-h exposures showed a mild increase in DNA damage at low and medium concentrations (23% and 49% relative increase, respectively), compared to the corresponding control. Interestingly, at the highest concentration, TI declined for both time points. This decrease may be associated with reduced cell viability; the more sensitive cells have undergone cell death, leaving a subpopulation of more resistant cells with relatively lower levels of measurable DNA damage (Flusberg and Sorger, 2015; Wang, 2019). Activation of DNA repair mechanisms may also contribute, particularly after 4 h of exposure, as this short exposure period may still allow effective repair responses (Azqueta et al., 2014, 2019). Although a similar trend was observed at

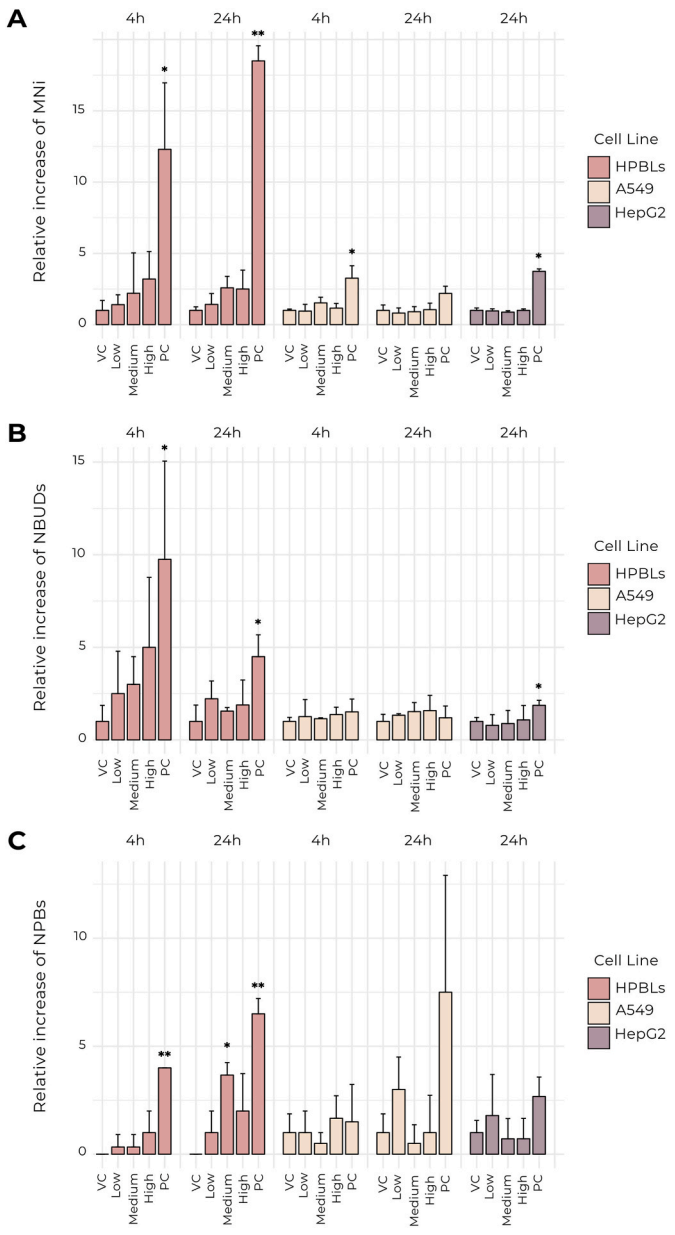

Fig. 6. Induction of cytogenetic damage in human peripheral blood lymphocytes (HPBLs), lung epithelial cells (A549), and hepatocellular carcinoma cells (HepG2) following exposure to a polycyclic aromatic hydrocarbons (PAHs) mixture, evaluated by cytokinesis-block micronucleus (CBMN) assay. HPBLs represent the proliferating lymphocyte fraction of peripheral blood cells used for CBMN analysis. (**A**) Relative increase in micronuclei (MNi), (**B**) nuclear buds (NBUDs), and (**C**) nucleoplasmic bridges (NPBs) per 1000 binucleated cells following exposure to low (1-h exposure scenario), medium (8-h exposure scenario), and high (16-h exposure scenario) concentrations of a PAHs mixture derived from indoor air monitoring in Zagreb (Croatia) households. CBMN assay data were analyzed using a quasi-Poisson distribution appropriate for count data. Due to deviations from parametric assumptions, the Kruskal–Wallis test was used, followed by Dunnett-type post hoc comparisons to identify differences from vehicle control. Positive controls (PC): bleomycin (10 μg/mL, HPBLs), 0.3 μg/mL etoposide (A549), and 0.1 μg/mL etoposide (HepG2). Vehicle control (VC; 0.1% DMSO) was used for all cell types. Data are presented as mean values +standard deviation (SD) of the relative increase over vehicle control. *$p < 0.05$, **$p < 0.01$.

both time points, the 24-h exposure in PBCs and A549 cells produced slightly higher TI values, though not statistically significant, which may indicate cumulative damage or reduced repair efficiency over time (Azqueta et al., 2019; Azqueta and Collins, 2013). Rodríguez-Romero et al. (2012) showed that individual PAHs (DahA, BghiP, BbF, and BaP) induced a concentration-dependent increase in DNA strand breaks and oxidative damage in HPBLs after 24h exposure, however, at much higher concentrations. Their stronger genotoxic responses, compared to our findings, likely arise from the use of individual PAH compounds at higher concentrations, whereas our study examined a real-life mixture at environmentally relevant levels without exogenous metabolic activation. However, consistent with our data in PBCs, they noted minimal cytotoxicity at lower concentrations. Notably, as discussed by Møller et al. (2025), even non-significant changes in comet assay endpoints may have biological importance, especially when seen consistently or in the context of other DNA damage markers. When treated with the same PAH mixture as PBCs, A549 and HepG2 cells exhibited a different genotoxic profile, likely due to differential xenobiotic-metabolizing capacity (Bosnjakovic et al., 2025). The comet assay results showed negligible DNA damage, which corresponded to the low frequency of MNi; nevertheless, the sensitivity of the alkaline comet assay allowed detection of even these subtle changes (Langie et al., 2015).

Beyond standard comet assay analysis, which is based on a specific algorithm or a combination of them (Bengtsson et al., 2004), we explored whether advanced image analysis could detect subtle exposure-related differences not captured by TI alone. Although classical and multifractal methods allow the extraction of numerous geometric, intensity, and texture features (Kraus and Frey, 2016), most descriptors in our dataset were redundant and showed no notable variation at 4 or 24 h under low and medium exposures, aligning with the weak TI response. Only the 24-h high-exposure condition produced measurable shifts in basic geometric parameters. Still, consistent time-dependent patterns were evident: 24-h images exhibited greater homogeneity, while 4-h images showed broader multifractal spectra and higher heterogeneity, indicating subtle structural reorganization of comet morphology even under low-damage conditions. Graph-based and topological metrics also showed potential, though multi-scale fractal dimension appeared more responsive to time than concentration (see Supplementary Material). Overall, these exploratory findings suggest that advanced image-derived metrics may detect nuanced DNA-damage-related patterns, but their current utility is limited by descriptor redundancy, preprocessing variability, and small sample size. Larger datasets will be needed to validate these trends and strengthen comet assay sensitivity.

The CBMN assay can assess genomic instability through the measurement of assay-specific parameters, which capture not only unrepaired DNA damage but also errors related to chromosome segregation and mitotic spindle dysfunction (Fenech, 2020; Fenech et al., 2011). In HPBLs, a concentration-dependent increase in MNi frequency was observed for both 4-h (3.2-fold increase at high concentration) and 24-h treatments (2.6-fold increase at medium concentration), as shown in Fig. 5A. Although the trend did not reach statistical significance, a three-fold increase compared to control may still indicate biologically relevant disruption of genome integrity in HPBLs. Meta-analysis by Nersesyan et al. (2016) has shown that exposure to known genotoxic chemicals such as benzene and PAHs produced approximately two-fold or greater increases in MN frequencies, highlighting biological relevance even when p-values do not pass conventional thresholds. MN elevation is likewise seen across many diseases, including cancers, indicating that meaningful genotoxic effects can occur below strict statistical cutoffs. Therefore, effect size and context (e.g., MN-mean ratio near or above 2 $\times$), not p-values alone, should guide precautionary interpretation and control measures (OECD, 2025). The 4-h treatment likely reflects clastogenic mechanisms (Fenech et al., 2020), as shown by slightly increased DNA strand breaks detected via the comet assay and the formation of MNi in the CBMN assay, which is further supported by the

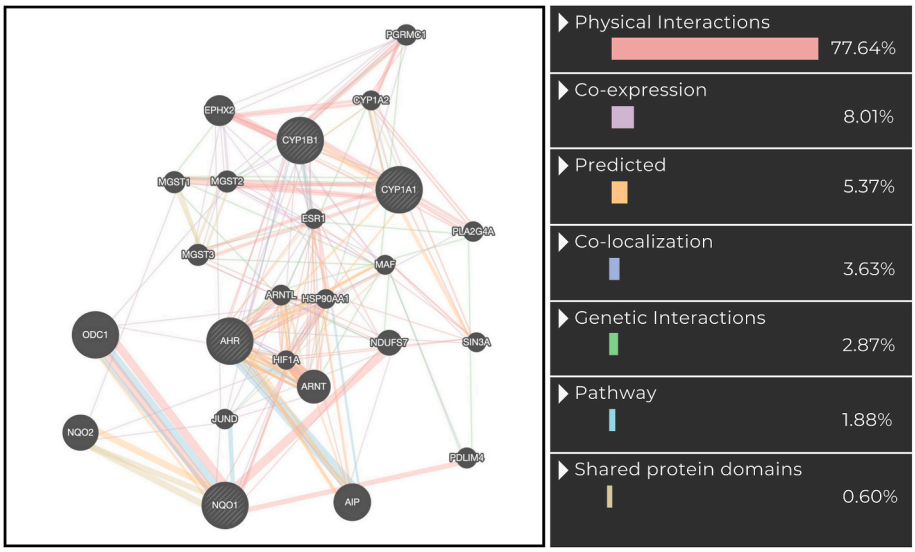

Fig. 7. Interaction network of genes common to the investigated PAHs [fluoranthene (Flu), pyrene (Pyr), benzo(a)anthracene (BaA), chrysene (Chry), benzo(b)fluoranthene (BbF), benzo(k)fluoranthene (BkF), benzo(a)pyrene (BaP), dibenzo(a,h)anthracene (DahA), benzo(ghi)perylene (BghiP), and indeno(1,2,3-cd)pyrene (IP)], together with 20 related genes (GeneMANIA (https://genemania.org)).

observation that HPBLs also showed an increase in both NBUDs (Fig. 6B) and NPBs (Fig. 6C). Notably, a statistically significant increase of NPBs was detected at the medium PAH concentration following 24-h treatment, where the frequency increased from 0 in control cells to 3.7. This finding suggests that, at longer exposure and environmentally relevant concentrations, PAHs may interfere with chromosome segregation or induce telomere end fusions, further compromising genomic stability in primary cells. These results also indicate that endpoints such as NBUDs and NPBs may serve as more sensitive indicators of PAH-induced genotoxicity than MNi alone, consistent with observations reported by Duan et al. (2009). In contrast, A549 and HepG2 cells showed no notable fold increase in any CBMN parameters. HepG2 cells demonstrated the minimal genotoxic response assessed by the comet assay after 24 h, with minimal DNA damage and correspondingly low MNi frequencies. Although both HepG2 and A549 cells showed overall negligible responses, A549 exhibited greater variability across replicates, whereas HepG2 displayed consistently low TI values, supporting the interpretation that genotoxic responsiveness was lowest in HepG2 under the tested conditions. The modest induction factors for MNi, despite higher basal frequencies typical of HepG2 cells, reinforce this conclusion. The minimal genotoxic effects observed in A549 and HepG2 cells suggest that the PAH concentrations, derived from median indoor air measurements in Zagreb, are below the threshold required to induce substantial DNA or chromosomal damage. This lack of response in A549 and HepG2 cells may reflect their greater metabolic competence and adaptive capacity (Foster et al., 1998; Madunić et al., 2022), enabling efficient biotransformation and repair of PAH-induced lesions during short-term exposure. The exposure durations used in this study may favor cellular detoxification and recovery mechanisms in immortalized cell lines, limiting the accumulation of persistent DNA or chromosomal damage. In line with this interpretation, Billet et al. (2008) demonstrated that relatively low doses of PM-bound PAHs significantly induced CYP1A1 gene expression and catalytic activity in A549 cells, yet under their experimental conditions did not result in reliably quantifiable PAH–DNA adduct formation, indicating effective metabolic activation without measurable accumulation of DNA damage. These findings therefore indicate that, under environmentally relevant and short-term exposure conditions, the tested PAH mixture does not elicit robust genotoxic effects in metabolically competent A549 and HepG2 cell models, highlighting the importance of exposure duration and cell-type-specific metabolism when interpreting largely negative *in vitro* outcomes. In HPBLs, the three-fold increase in MNi and statistically significant rise in NPBs indicate a detectable but still moderate biological response, particularly when considering the absence of consistent significance across concentrations. This pattern suggests that the tested 11-PAH mixture, designed to mimic real-scenario indoor exposure, possesses limited potential to elicit a robust genotoxic effect under these short-term exposure conditions.

Previous studies examining the cytotoxic and genotoxic potential of PAH mixtures have shown considerable variability in their outcomes, largely driven by differences in cell models, mixture composition, and higher exposure concentrations, often revealing non-additive or antagonistic effects. However, most of that research relied on simplified binary or small-component mixtures and did not incorporate real-life exposure scenarios, highlighting the distinctiveness of the present study, which employs a complex, environmentally derived 11-PAH mixture across three human-relevant cell models. Castel et al. (2023) investigated six PAHs in adherent human adenocarcinoma gastric (AGS) cells and found mostly antagonistic interactions for chromosomal damage endpoints, though some high-molecular-weight PAH pairs (e.g. BaP with BbF) showed synergistic DNA damage. These findings partially align with our results, particularly in PBCs, where we observed a slight, concentration-dependent increase in DNA and chromosomal damage at moderate concentrations but not at the highest, possibly reflecting a similar interplay of metabolic saturation or repair mechanisms. Muthusamy et al. (2018) demonstrated that co-exposure of BaP with metals or other PAHs reduced genotoxicity, likely due to competition at the aryl hydrocarbon receptor (AHR), which can hinder BaP activation. These findings are partly consistent with our results, where we observed low DNA and chromosomal damage in HepG2 cells, possibly due to similar metabolic detoxification or receptor-mediated interactions in the presence of multiple PAHs. Gaskill and Bruce (2016) reported predominantly antagonistic effects of PAH mixtures in normal rat liver Clone-9 cells, noting that many combinations inhibited BaP-induced genotoxicity due to overlapping metabolic or elimination pathways. This aligns with our observation of low genotoxic outcomes in transformed cell lines like A549 and HepG2 cells and modest effects in PBCs, suggesting that complex mixture effects may dampen or modulate the overall genotoxic response to individual components.

The muted biological responses observed across our *in vitro* models may be explained by the composition of the PAH mixture and its toxic equivalency factor (TEF)-weighted potency (Nisbet and LaGoy, 1992).

Table 3
Results of the functional analysis of the genes common to the investigated PAHs [fluoranthene (Flu), pyrene (Pyr), benzo(a)anthracene (BaA), chrysene (Chry), benzo (b)fluoranthene (BbF), benzo(k)fluoranthene (BkF), benzo(a)pyrene (BaP), dibenzo(a,h)anthracene (DahA), benzo(ghi)perylene (BghiP), and indeno(1,2,3-cd)pyrene (IP)], presented through their molecular functions, biological processes, cellular components, molecular pathways, and associated diseases (ToppGene Suite (https://toppgene.cchmc.org)).

Category	ID	Name	p-value	Gene Number
Molecular functions	GO:0016712	oxidoreductase activity, acting on paired donors, with incorporation or reduction of molecular oxygen, reduced flavin or flavoprotein as one donor, and incorporation of one atom of oxygen	7.882E-8	3
	GO:0106256	hydroperoxy icosatetraenoate dehydratase activity	6.312E-7	2
	GO:0004497	monooxygenase activity	1.097E-6	3
	GO:0101021	estrogen 2-hydroxylase activity	1.653E-6	2
	GO:0016491	oxidoreductase activity	1.878E-6	4
	GO:0101020	estrogen 16-alpha-hydroxylase activity	1.983E-6	2
	GO:0016705	oxidoreductase activity, acting on paired donors, with incorporation or reduction of molecular oxygen	4.480E-6	3
	GO:0008395	steroid hydroxylase activity	1.785E-5	2
	GO:0016709	oxidoreductase activity, acting on paired donors, with incorporation or reduction of molecular oxygen, NAD(P)H as one donor, and incorporation of one atom of oxygen	4.129E-5	2
	GO:0051879	Hsp90 protein binding	4.449E-5	2
Biological processes	GO:1904681	response to 3-methylcholanthrene	1.105E-11	3
	GO:1903165	response to polycyclic arene	1.105E-11	3
	GO:0097267	omega-hydroxylase P450 pathway	1.257E-9	3
	GO:0006805	xenobiotic metabolic process	2.950E-9	4
	GO:0071466	cellular response to xenobiotic stimulus	1.874E-8	4
	GO:0072593	reactive oxygen species metabolic process	4.329E-8	4
	GO:1901654	response to ketone	4.447E-8	4
	GO:0009636	response to toxic substance	6.846E-8	4
	GO:0019369	arachidonate metabolic process	1.261E-7	3
	GO:0018894	dibenzo-p-dioxin metabolic process	4.259E-7	2
Cellular components	GO:0034752	cytosolic aryl hydrocarbon receptor complex	1.916E-4	1
	GO:0034753	nuclear aryl hydrocarbon receptor complex	3.831E-4	1
	GO:0034751	aryl hydrocarbon receptor complex	1.532E-3	1
Pathway	M39615	aryl hydrocarbon receptor pathway	8.676E-11	4
	M39661	aryl hydrocarbon receptor pathway	9.502E-11	4
	M47513	AHR signaling pathway	4.644E-10	3
	M39424	estrogen metabolism	6.764E-9	3
	MM15888	estrogen metabolism	1.276E-8	3
	M47806	env factor TCDD to AHR signaling pathway	1.468E-8	3
	M39428	nuclear receptors metapathway	2.314E-7	4
	M5650	cytochrome P450 arranged by substrate type	3.445E-7	3
	MM14839	cytochrome P450 arranged by substrate type	3.784E-7	3
	MM14856	synthesis of epoxy EET and dihydroxyeicosatrienoic acids DHET	1.241E-6	2
Disease	C0162351	contact hypersensitivity	3.073E-11	4
	C0011616	contact dermatitis	3.073E-11	4
	C0019209	hepatomegaly	2.312E-8	3
	C0242706	hyperoxia	4.132E-8	2
	C1383860	cardiac hypertrophy	8.250E-8	3
	C0018800	cardiomegaly	8.250E-8	3
	C1257931	mammary neoplasms, human	9.897E-8	4
	C4704874	mammary carcinoma, human	9.897E-8	4
	C1458155	mammary neoplasms	1.005E-7	4
	C0678222	breast carcinoma	1.092E-7	4

While highly potent PAHs such as DahA (TEF = 5) and BaP (TEF = 1) were present, they contributed only 1.4% and 9.8% to the total PAH mixture, respectively. In contrast, the most abundant compounds, IP and BghiP, accounted for more than 30% combined, but have very low TEFs (0.1 and 0.01). Similarly, Flu and Pyr (TEF = 0.001 each) added an additional 18%, further lowering the overall toxic potency (Nisbet and LaGoy, 1992). Tomasetig et al. (2020) investigated the genotoxic potential of 27 PAHs using three human cell lines (hepatoma (Hep3B) cells, epithelial colorectal adenocarcinoma (LS-174T) cells, and bronchioalveolar carcinoma (NCI-H358) cells), establishing genotoxic equivalent factors (GEFs) relative to BaP (GEF = 1) after 24-h exposure. Of the 11 PAHs used in our indoor air-derived mixture, six, including Flu, Pyr, Chry, BkF, BghiP, and IP, were reported to have no measurable or relatively low genotoxic potential in any of the three cell lines. Conversely, PAHs such as BaP, BbF, BjF, and BaA demonstrated low to moderate GEFs, while DahA exhibited the highest GEF values, particularly in Hep3B (GEF = 1.87) and NCI-H358 cells (GEF = 2.77). However, DahA was the least abundant compound in our indoor air mixture. PAHs with the highest measured indoor concentrations, such as IP, BghiP, and BbF, were either non-genotoxic or exhibited low GEFs, suggesting a weaker overall genotoxic burden. When compared with previously published TEFs by Nisbet and LaGoy (1992), these GEFs provide a more cell-type-specific, mechanistically relevant context for interpreting *in vitro* responses. These comparisons support our *in vitro* results, where modest cytogenetic effects were observed. Taken together, the GEF data reinforce the idea that the qualitative composition and toxic potency,

Table 4
Results of the functional analysis of the cumulative set of genes interacting with the examined PAHs (fluoranthene (Flu), pyrene (Pyr), benzo(a)anthracene (BaA), chrysene (Chry), benzo(j)fluoranthene (BjF), benzo(b)fluoranthene (BbF), benzo(k)fluoranthene (BkF), benzo(a)pyrene (BaP), dibenzo(a,h)anthracene (DahA), benzo (ghi)perylene (BghiP), and indeno(1,2,3-cd)pyrene (IP)), presented through their molecular functions, biological processes, cellular components, molecular pathways, and associated diseases (ToppGene Suite (https://toppgene.cchmc.org)).

Category	ID	Name	p-value	Gene Number
Molecular functions	GO:0046873	metal ion transmembrane transporter activity	2.884E-23	561
	GO:0030554	adenyl nucleotide binding	5.440E-21	1550
	GO:0005215	transporter activity	9.675E-21	1334
	GO:0032559	adenyl ribonucleotide binding	1.633E-18	1436
	GO:0005102	signaling receptor binding	4.666E-18	1604
	GO:0022836	gated channel activity	8.095E-18	330
	GO:0005524	ATP binding	3.170E-17	1388
	GO:0019904	protein domain specific binding	3.676E-17	809
	GO:0022857	transmembrane transporter activity	8.463E-17	1208
	GO:0008289	lipid binding	1.331E-16	927
Biological process	GO:0007267	cell-cell signaling	4.020E-60	1536
	GO:0007155	cell adhesion	9.627E-51	1580
	GO:0060429	epithelium development	1.818E-46	1424
	GO:0048699	generation of neurons	3.250E-45	1752
	GO:0009887	animal organ morphogenesis	5.584E-44	1207
	GO:0030182	neuron differentiation	2.849E-43	1671
	GO:0034330	cell junction organization	7.937E-41	970
	GO:0009967	positive regulation of signal transduction	9.514E-41	1731
	GO:0016310	phosphorylation	4.498E-40	1347
	GO:0046903	secretion	8.647E-39	1184
Cellular components	GO:0098590	plasma membrane region	5.766E-65	1513
	GO:0043005	neuron projection	1.300E-51	1599
	GO:0036477	somatodendritic compartment	7.691E-42	1181
	GO:0098978	glutamatergic synapse	3.206E-40	841
	GO:0070161	anchoring junction	7.234E-40	942
	GO:0030424	axon	2.005E-36	860
	GO:0098794	postsynapse	5.776E-36	1016
	GO:0009986	cell surface	8.639E-35	1052
	GO:0097447	dendritic tree	1.035E-34	836
	GO:0030425	dendrite	1.435E-34	834
Pathway	M27451	metabolism of lipids	3.797E-18	727
	M610	extracellular matrix organization	5.299E-17	319
	M27287	transport of small molecules	1.584E-15	691
	MM14572	extracellular matrix organization	1.114E-14	279
	M39428	nuclear receptors metapathway	2.602E-14	310
	M39729	VEGFA-VEGFR2 signaling	1.056E-13	419
	MM15193	metabolism of lipids	1.124E-12	590
	M746	signaling by GPCR	3.002E-12	666
	M27870	signaling by receptor tyrosine kinases	1.236E-11	509
	M12868	pathways in cancer	2.225E-11	317
Disease	C0006142	malignant neoplasm of breast	5.575E-154	996
	C0023893	liver cirrhosis, experimental	1.239E-150	752
	C0036341	schizophrenia	2.054E-123	816
	C0009402	colorectal carcinoma	1.742E-109	660
	C0376358	malignant neoplasm of prostate	6.459E-105	587
	C0033578	prostatic neoplasms	6.459E-105	587
	C2239176	liver carcinoma	2.264E-92	488
	C0005586	bipolar disorder	9.057E-87	459
	C0678222	breast carcinoma	2.681E-70	492
	C1458155	mammary neoplasms	7.674E-70	483

rather than the mere presence or quantity of PAHs, are critical determinants of their biological impact under environmentally relevant exposure conditions.

Although genotoxic compounds are generally regarded as non-threshold agents, meaning that even very low exposures may carry some degree of risk, the compositional characteristics of the mixture, combined with the relatively short exposure durations (1, 8, and 16 h), resulted in *in vitro* concentrations far below typical occupational exposure levels (Jang et al., 2018). However, it is important to bear in mind that occupational exposure limits are regulatory values intended to indicate levels of exposure in workplace air that are considered safe. Their primary purpose is to protect workers' health by limiting exposure to hazardous chemicals encountered in occupational settings. They are mainly designed to prevent inhalation exposure to chemicals in the form of vapors, mists, or dusts, as well as to provide protection against dermal exposure (ECHA, 2026). Although occupational exposure limits are established by many countries and professional organizations, substantial differences exist in both the derivation methodologies and the resulting limit values. In recent years, efforts have been undertaken to move toward a more globally harmonized approach, notably within the framework of the OECD (2022). The lowest regulatory threshold for occupational exposure to coal tar pitch volatiles, which encompass various PAHs, is set by the National Institute for Occupational Safety and Health (NIOSH) at 0.1 mg/m^3 (or 100,000 ng/m^3) as an 8-h time-weighted average (TWA) (NIOSH, 2014). Recently, in light of the latest scientific evidence, the European Commission launched a proposal to amend Directive 2004/37/EC on the protection of workers from the risks related to exposure to carcinogens or mutagens at work, by adding new substances and setting corresponding limit values, including an occupational exposure limit for BaP of 0.00007 mg/m^3 for an 8-h TWA (European Commission, 2026). When considering exposure to PAHs outside the workplace atmosphere, particularly in indoor ambient air, the WHO emphasizes that no safe threshold can be determined and that all indoor exposures are considered relevant to human health. Owing to

the difficulties in developing guideline values for complex PAH mixtures, the WHO continues to regard BaP as the most appropriate single indicator compound (Choi H et al., 2010). In its assessment, the WHO concluded that occupational epidemiological data should form the basis for risk estimation. On the basis of epidemiological studies conducted among coke-oven workers, a unit risk for lung cancer associated with PAH mixtures was estimated to be 8.7×10^{-5} per ng/m^3 of BaP. Accordingly, the estimated BaP concentrations corresponding to excess lifetime cancer risks of 1 in 10,000, 1 in 100,000, and 1 in 1,000,000 are approximately 1.2, 0.12, and 0.012 ng/m^3, respectively, assuming lifetime exposure (WHO, 2000). The WHO further notes that the application of the BaP unit risk factor assumes that BaP accounts for a similar proportion of the carcinogenic activity of PAH mixtures in indoor environments as it does in occupational settings. Although this assumption may not always be valid, the resulting uncertainties in risk estimates are not expected to be substantial. As BaP is consistently present in PAH mixtures, reducing exposure to BaP may also contribute to a reduction in the risk of other adverse health effects associated with PAHs (Choi H et al., 2010; WHO, 2000). Considering the concentrations of individual PAHs measured in our study, median residential indoor air samples ranged from 0.015 to 0.177 ng/m^3, with a BaP median value of 0.102 ng/m^3. This means that indoor household PAH exposures in our study were at least five to six orders of magnitude lower than the lowest occupational exposure limit. Such a substantial difference highlights the considerably lower risk associated with residential indoor air, emphasizing that the measured PAH levels in our study fall not only far below any occupational safety thresholds, but also indicate relatively low risk considering even WHO risk estimations regarding potential effects under long-term, low-dose exposure. While such comparisons cannot be used to establish a “safe” level for genotoxic compounds, they do contextualize the relatively muted responses observed *in vitro*. Consistent with this, the comet assay, which detects early, repairable DNA lesions, revealed nonsignificant damage across all three cell types (Azqueta and Collins, 2013; Collins et al., 2014, 2023; Møller, 2018). Nonetheless, the 2–3-fold increase in MNi and the significant rise in NPBs in HPBLs at the highest exposure scenario indicate that even low-level, environmentally relevant mixtures may induce subtle chromosomal instability detectable by the CBMN assay. Our interpretation is further supported by a recent air quality study in Zagreb, which found lower PAH concentrations indoors compared to outdoors, and estimated incremental lifetime cancer risks for residents to be below U.S. EPA safety thresholds (Lovrić et al., 2024). These findings affirm that indoor PAH exposures in this region currently pose limited genotoxic risk under typical living conditions but highlight the importance of considering both the qualitative composition of PAH mixtures and their TEF- and GEF-weighted toxic potential. In line with the review by Račić et al. (2025), the indoor PM-bound PAH concentrations measured in Zagreb households fall at the lower end of values reported across Europe, while exhibiting a compositional profile comparable to other urban environments. Within this context, qualitative benchmarking indicates that the summed median concentration of 11 PM_1-bound PAHs in the present study (≈1.06 ng/m^3) is lower than totals commonly reported for $PM_{2.5}$-bound PAHs in European homes, which often reach several ng/m^3 or higher. Despite these quantitative differences, similar combustion-related source signatures and seasonal patterns are observed across regions, supporting the broader applicability of our findings to mid-sized European cities where indoor exposure is primarily driven by outdoor infiltration and routine household activities. Sustained PAH monitoring and public awareness are critical, as well as targeted mitigation strategies aimed at reducing the presence of these compounds in indoor environments, particularly given that the highest percentage of detected PAHs were those typically associated with car exhaust emissions, including BbF, BghiP, and IP, which persist throughout the year (Jakovljević et al., 2020).

This study's main strengths include the use of indoor air-derived, environmentally relevant PAH concentrations and the evaluation of a complex 11-PAH mixture across three human-relevant cell models. Together, these features offer a more realistic assessment of PAH mixture toxicity compared with conventional studies relying on simplified mixtures or high experimental doses. The modest biological responses observed in our study likely reflect this lower exposure magnitude, highlighting the translational value and the relevance of our findings. However, this approach may also limit the detection of effects that only manifest at higher exposure levels. While conventional two-dimensional (2D) cell cultures provide valuable insights into cytotoxic and genotoxic effects and remain widely used in toxicological research, emerging three-dimensional (3D) culture systems offer complementary advantages. By better recapitulating tissue architecture, cell–cell interactions, and metabolic functionality, 3D models can provide a more physiologically relevant context for assessing xenobiotic metabolism and complex mixture effects (Wrzesinski and Fey, 2018). Integrating 3D cultures in future studies could enhance our understanding of systemic and organ-specific responses to PAH mixtures that are not fully captured in static 2D systems, thereby building upon the mechanistic insights obtained from established 2D models (Štampar et al., 2021; Štampar and Žegura, 2024).

4.3. *In silico toxicogenomic data analysis*

To complement the experimental findings and further explore mechanisms of toxicity of environmentally relevant PAHs, *in silico* toxicogenomic analysis was conducted. While the *in vitro* segment of the present study captures immediate cellular effects, computational profiling provides a broader mechanistic perspective, identifying shared molecular targets (genes and proteins), gene ontology (molecular functions, biological processes, cellular components), pathway disruptions, and connected diseases. A recent study by Abu-Bakar et al. (2024) used *in silico* toxicogenomic data-mining of 25 carcinogenic hydrocarbons (alkanes, alkenes, halogenated hydrocarbons, and PAHs - BaP and anthracene) to identify shared gene interactions and pathways, showing that these pollutants converge on oxidative stress, inflammatory signaling, and ferroptosis-related mechanisms, particularly through a core set of 16 genes linked to both breast and lung cancer. However, to the best of our knowledge, no *in silico* study to date has examined a mixture comprising the specific 11 PAHs included in our investigation. Thus, by examining a defined mixture of 11 PAHs and integrating *in vitro* findings with *in silico* mechanistic profiling, our study fills this gap and provides a more realistic and comprehensive view of how the PAH mixture perturbs cellular pathways. Analysis revealed overlapping gene profiles across all 11 PAHs in the mixture, with *AHR*, *CYP1A1*, and *CYP1B1* being common to every compound. AHR, a ligand-activated transcription factor, regulates the expression of detoxification and metabolic genes. Upon ligand binding, AHR translocates to the nucleus and induces transcription of xenobiotic-metabolizing enzymes such as CYP1A1, the best-characterized downstream target of this pathway (Zhang et al., 2025). CYP1A1 and CYP1B1 enzymes play essential roles in metabolizing both environmental chemicals and endogenous molecules, making them central to AHR-driven toxicity, cancer development, hormonal and lipid regulation, as well as individual variation in drug response (Kwon et al., 2021). *NQO1* was shared among all PAHs except BjF, highlighting activation of a major phase II detoxification pathway via NAD(P)H:quinone oxidoreductase (Valerio et al., 2001). The *NQO1*-encoded enzyme is a widely expressed FAD-dependent oxidoreductase that performs two-electron reductions of quinones and related substrates, thereby suppressing redox cycling and oxidative stress. Its expression is highly inducible and mainly controlled by the Keap1–Nrf2–ARE antioxidant pathway (Dinkova-Kostova and Talalay, 2010). The majority of interactions among these mutual genes (77.6%) were physical, followed by co-expression (8.0%), with the remaining interactions predicted by the GeneMANIA server or based on co-localization. This highlights the strong interconnection of these genes and the central role of the AHR–CYP–NQO1 axis in the toxicity of the investigated PAHs mixture. Functional analysis of these four genes

common to all investigated PAHs showed predominant roles in oxidative metabolism and xenobiotic biotransformation, including oxidoreductase, monooxygenase, and hydroxylase activities, as well as interactions with Hsp90, heat shock protein which forms part of a chaperone complex that binds and stabilizes AHR in the cytosol until ligand binding triggers AHR release and nuclear translocation to activate target genes (Heid et al., 2000). Extracted biological processes have shown that the investigated common genes mediate responses to xenobiotics, toxic substances, polycyclic arenes, and reactive oxygen species. Expectedly, pathway analysis confirmed the dominance of AHR signaling, cytochrome P450-mediated metabolism, and downstream estrogen hydroxylation, with CYP1B1-mediated catechol estrogen formation providing a mechanistic link to endocrine disruption. Enrichment of cytosolic and nuclear AHR complexes further validates AHR activation and translocation. Disease associations included immune and inflammatory conditions such as contact hypersensitivity and dermatitis, systemic effects like hepatomegaly and cardiac hypertrophy, and hormone-related cancers, particularly mammary neoplasms and breast carcinoma.

While the analysis of mutual genes highlighted a narrow AHR–CYP–NQO1 axis, the broader cumulative gene set demonstrates that PAHs engage an extensive network of molecular targets across multiple cellular systems. Molecular functions such as metal ion and transmembrane transport, gated channel activity, ATP and nucleotide binding, signaling receptor binding, protein domain-specific binding, and lipid interactions indicate roles in energy-dependent transport, enzymatic activity, signal transduction, and molecular recognition. The associated biological processes emphasize intercellular communication, tissue organization, and neuronal development, including cell-cell signaling, cell adhesion, epithelium development, neuron differentiation, and generation of neurons. Processes like phosphorylation, secretion, and positive regulation of signal transduction highlight intracellular signaling and molecular communication. Extracted cellular components such as plasma membrane, cell surface, junctions, and neuronal structures such as axons, dendrites, dendritic trees, somatodendritic compartments, and glutamatergic synapses reflect their involvement in mediating both structural integrity and functional connectivity. These molecular functions, biological processes, and cellular components indicate that PAHs affect not only metabolic pathways but also broader developmental, signaling, and synaptic mechanisms, with potential impacts on tissue morphology, neuronal function, and cellular homeostasis. The pathway analysis for the cumulative set of PAH-interacting genes suggests their involvement in metabolic, signaling, and regulatory functions. Enriched pathways such as metabolism of lipids and transport of small molecules indicate roles in cellular homeostasis and xenobiotic handling, while extracellular matrix organization points to functions in tissue structure, adhesion, and remodeling. Signaling pathways, including nuclear receptor metapathways, GPCR signaling [G-protein coupled receptors (GPCRs), the largest family of membrane receptors, transduce diverse extracellular signals through G proteins and secondary messengers, enabling broad regulation of cellular metabolism and physiological responses (Cho et al., 2025)], receptor tyrosine kinase signaling, and VEGF/VEGFR2 signaling [VEGF-A, through its primary receptor VEGFR2, regulates angiogenesis by promoting endothelial cell proliferation, migration, survival, and new vessel formation (Abhinand et al., 2016)], emphasize that these genes mediate intercellular communication, hormonal regulation, and angiogenic responses. The enrichment in “pathways in cancer” reflects their potential contribution to oncogenic processes. Hence, disease associations have indicated that multiple cancer types, including breast, prostate, colorectal, and liver neoplasms, might be connected to the investigated PAHs mixture. Associations with liver cirrhosis suggest involvement in organ stress, whereas links to neuropsychiatric disorders such as schizophrenia and bipolar disorder indicate potential effects on neuronal development. Taken together, the *in silico* results of the current study suggest that the investigated PAHs mixture activates multiple metabolic and systemic mechanisms, clarifying the molecular basis of their varied toxic effects.

In summary, the *in silico* toxicogenomic analysis enabled the identification of the dominant molecular pathways associated with exposure to the investigated PAH mixture. While the cumulative gene set interacting with PAHs was extensive and enriched for diverse signaling, developmental, and disease-related pathways, analysis of genes shared across all compounds revealed a highly focused mechanistic signature. This signature was dominated by activation of AHR and its downstream targets CYP1A1, CYP1B1, and NQO1, underscoring AHR-driven xenobiotic metabolism and redox regulation as the central molecular response to PAH exposure. The overrepresentation of monooxygenase activity, cytochrome P450–mediated metabolism, and oxidative stress–related biological processes supports metabolic activation as a key initiating event underlying PAH toxicity. In contrast, pathways identified within the broader cumulative gene set, such as lipid metabolism, receptor-mediated signaling, extracellular matrix organization, angiogenesis, and cancer-related processes, likely reflect secondary, tissue-specific, and systemic consequences of sustained PAH–gene interactions rather than primary drivers of toxicity. These findings provide a coherent mechanistic framework that contextualizes the *in vitro* results and links PAH exposure to oxidative, endocrine, inflammatory, and oncogenic outcomes. However, although our *in silico* investigation has indicated that AHR–CYP1A1/CYP1B1–NQO1 axis is shared by all investigated PAHs, the toxicological outcomes in our *in vitro* study differed markedly among the three cell models, reflecting pronounced cell-type–specific differences. *CYP1A1*, *CYP1B1* and *NQO1* genes (encoding cytochromes P450 1A1, 1B1, and NAD(P)H:quinone oxidoreductase 1, respectively) are all regulated by AHR (Grishanova and Perepechaeva, 2022). All of these enzymes play roles in both the detoxification and metabolic activation of a range of endogenous and foreign compounds, including PAHs (Dong et al., 2013). CYP1A1 and CYP1B1 are crucial for converting PAHs into epoxide intermediates, which epoxide hydrolase then transforms into the ultimate carcinogenic diol-epoxides (Shimada and Fujii-Kuriyama, 2004). NQO1 is a key cellular defense enzyme that detoxifies reactive quinones and quinone imines into less harmful hydroquinones (Atia and Abdullah, 2020). The toxic effects of PAHs are mainly influenced by metabolic activation and AhR-dependent transcription, with HepG2 cells exhibiting more efficient AHR signaling than A549 cells, likely due to their hepatic origin and higher receptor levels (Castorena-Torres et al., 2008). In the current study, HepG2 cells did not show significant cytotoxicity, DNA damage, or genomic instability after exposure to the 11-PAH mixture, even though these cells are known to have active metabolic pathways. This indicates that strong activation of the AHR in liver cells does not always lead to increased genotoxic effects under the conditions tested. One possible explanation is that AHR can bind many different ligands, often with low affinity, and at the same time trigger detoxification enzymes that break down these compounds. This creates a self-limiting, cell--specific response (Denison and Nagy, 2003). In contrast, A549 cells showed modest decreases in viability and subtle increases in DNA damage and micronucleus formation. A549 cells retain inducible expression of key pulmonary CYP enzymes involved in PAH metabolism, particularly CYP1A1 and CYP1B1, but lack broad xenobiotic-metabolizing capacity (Hukkanen et al., 2000), which is consistent with the modest cytotoxic and genotoxic responses observed in A549 cells following PAH mixture exposure in the present study. Genies et al. (2013) support our findings of cell-type–specific PAH responses: HepG2 cells showed minimal genotoxic effects despite metabolic activation, while A549 cells exhibited limited, non-linear responses. Rossner et al. (2016) showed that A549 cells respond differently to individual PAHs: 3-NBA was the most potent genotoxicant, while 1-NP primarily induced oxidative stress, reflected by AKR1C2 and COX2 expression. Unlike BaP, nitro-PAHs weakly induced AHR-mediated CYP1A1/1B1 expression, though all compounds increased NQO1, POR, and AKR1C2. Hence, it is possible that in our

study, exposure to a mixture of 11 PAHs caused only modest cytotoxic and genotoxic effects in A549 cells due to interactions and suppression of highly active components of the investigated mixture. As mentioned before, PBMCs have limited PAH detoxification capacity compared with hepatic and A549 cells. Accordingly, human biomonitoring studies consistently report elevated DNA strand breaks, oxidative lesions, and chromosomal damage (e.g., MNi and sister chromatid exchanges) in PBCs of PAH-exposed individuals compared with controls (Andersen et al., 2018). PAHs modulate immune cell function via CYP-mediated bioactivation, inducing oxidative and electrophilic stress that disrupts lymphocyte signaling and promotes DNA damage and apoptosis (Burchiel and Luster, 2001). This is consistent with our finding that primary blood cells showed the strongest cytotoxic and genotoxic responses to the 11-PAH mixture.

5. Conclusion

What distinguishes our study is the use of a complex, environmentally relevant PAH mixture reflective of average indoor air quality in residential Zagreb settings in Croatia. Overall, the indoor PM_1-bound PAH concentrations measured in Zagreb households lie at the lower end of values reported across Europe, while exhibiting a compositional profile comparable to other urban settings, indicating a relatively low indoor PAH burden and positioning Zagreb as a representative reference for mid-sized European cities where indoor exposure is predominantly driven by outdoor infiltration and routine household activities. While many previous studies have provided valuable insights using BaP-centered binary or simplified PAH mixtures, our approach captures the broader complexity of real-life indoor exposures. By integrating three human-derived cell systems, blood, lung (A549), and liver cells (HepG2), we were able to assess both systemic and cell-specific responses across biologically distinct models. The observed muted cytogenetic outcomes likely reflect not only the low concentrations used, but also the dominance of PAHs with limited or no genotoxic potential based on both TEF and GEF metrics. Our findings showed no substantial cytotoxic or genotoxic effects across any of the tested lines, with only PBMCs showing notable cytotoxicity that did not translate to widespread DNA and chromosomal damage in A549 or HepG2 cells. The results underscore the importance of cell-type specificity when assessing genotoxic effects of PAHs, suggesting that PAH-induced cytotoxicity and genotoxicity are both concentration- and time-dependent, with cellular metabolism, DNA repair capacity, and survival mechanisms playing critical roles in modulating outcomes. Particularly, the balance between DNA damage induction and repair determines whether damage is resolved or progresses into chromosomal aberrations. Taken together, our data support the relevance of integrating multiple endpoints (viability, DNA damage, and chromosomal damage) across different cell types to comprehensively evaluate the risk posed by complex indoor PAH mixtures. The *in silico* analysis further indicated that the toxicity of the investigated PAH mixture is largely driven by the AHR–CYP–NQO1 axis, with strong connections between the shared genes (*AHR*, *CYP1A1*, *CYP1B1*, and *NQO1*) and pathways involved in xenobiotic metabolism and oxidative stress. Moreover, the broader gene set indicated that PAHs affect many other cellular processes, including metabolism, signaling, development, and neuronal function, providing a mechanistic basis for their diverse toxic effects. Importantly, this study highlights the translational relevance of using environmentally realistic PAH mixtures at low concentrations, demonstrating that current indoor exposure levels in residential settings may pose limited genotoxic risk under typical conditions. Overall, our findings emphasize the value of integrating experimental and computational approaches to better understand the mechanisms of complex chemical mixture toxicity.

CRediT authorship contribution statement

Luka Kazensky: Writing – review & editing, Writing – original draft, Visualization, Investigation, Formal analysis. **Marija Jelena Lovrić Štefiček:** Writing – review & editing, Investigation. **Vilena Kašuba:** Writing – review & editing, Investigation. **Matjaž Novak:** Writing – review & editing, Investigation, Formal analysis. **Karolina Belingar:** Writing – review & editing, Investigation. **Katarina Matković:** Writing – review & editing, Writing – original draft, Visualization, Formal analysis. **Marko Gerić:** Writing – review & editing, Writing – original draft, Supervision, Project administration, Investigation, Conceptualization. **Jasmina Rinkovec:** Writing – review & editing, Investigation. **Ivana Jakovljević:** Writing – review & editing, Investigation, Formal analysis. **Katarina Baralić:** Writing – review & editing, Supervision, Resources, Investigation, Formal analysis. **Danijela Đukić-Ćosić:** Writing – review & editing, Supervision, Resources, Investigation, Formal analysis. **Mirta Milić:** Writing – review & editing, Investigation. **Želimir Jelčić:** Writing – review & editing, Visualization, Investigation, Formal analysis. **Gordana Pehnec:** Writing – review & editing, Supervision, Resources, Project administration, Funding acquisition, Conceptualization. **Bojana Žegura:** Writing – review & editing, Supervision, Resources, Project administration, Funding acquisition, Conceptualization. **Goran Gajski:** Writing – review & editing, Writing – original draft, Supervision, Resources, Project administration, Methodology, Investigation, Funding acquisition, Formal analysis, Conceptualization.

Declaration of competing interest

The authors declare that they have no known competing financial interests or personal relationships that could have appeared to influence the work reported in this paper.

Acknowledgments

The authors express their gratitude to Maja Nikolić for her invaluable technical assistance. This research was funded by the affiliated institutions, the European Union's Horizon Europe research and innovation program (EDIAQI project #101057497), the Croatian Science Foundation (HUMNap project #1192), the Foundation of the Croatian Academy for Science and Arts, the European Regional Development Fund project KK.01.1.January 1, 0007 “Research and Education Centre of Environmental Health and Radiation Protection,” the European Union – Next Generation EU (#533-03-23-0006, BioMolTox and EnvironPollutHealth), the Ministry of Science, Technological Development and Innovation, Republic of Serbia (#451-03-136/2025-03/200161), the Slovenian Research Agency (#P1-0245), and the bilateral collaborations between the Republic of Croatia and the Republic of Slovenia (MULTIap project #BI-HR/25-27-014). The city map used in Fig. 1 was generated using Snazzy Maps.

Appendix A. Supplementary data

Supplementary data to this article can be found online at https://doi.org/10.1016/j.envres.2026.124252.

Data availability

Data will be made available on request.

References

Abdel-Shafy, H.I., Mansour, M.S.M., 2016. A review on polycyclic aromatic hydrocarbons: source, environmental impact, effect on human health and remediation. Egypt. J. Pet. 25, 107–123. https://doi.org/10.1016/J.EJPE.2015.03.011.

Abhinand, C.S., Raju, R., Soumya, S.J., Arya, P.S., Sudhakaran, P.R., 2016. VEGF-A/VEGFR2 signaling network in endothelial cells relevant to angiogenesis. J. Cell Commun. Signal. 10, 347–354. https://doi.org/10.1007/s12079-016-0352-8.

Abu-Bakar, A., Ismail, M., Zulkifli, M.Z.I., Zaini, N.A.S., Shukor, N.I.A., Harun, S., Inayat-Hussain, S.H., 2024. Mapping the influence of hydrocarbons mixture on molecular

mechanisms, involved in breast and lung neoplasms: in silico toxicogenomic data-mining. Gene Environ. 46 (1 46), 2024. https://doi.org/10.1186/S41021-024-00310-Y.

Alley, M.C., Scudiere, D.A., Monks, A., Hursey, M.L., Czerwinski, M.J., Fine, D.L., Abbott, B.J., Mayo, J.G., Shoemaker, R.H., Boyd, M.R., 1988. Feasibility of drug screening with panels of human tumor cell lines using a microculture tetrazolium Assay1. Cancer Res. 48, 89–90.

Andersen, M.H.G., Saber, A.T., Clausen, P.A., Pedersen, J.E., Løhr, M., Kermanizadeh, A., Loft, S., Ebbehøj, N., Hansen, Å.M., Pedersen, P.B., Koponen, I.K., Nørskov, E.C., Møller, P., Vogel, U., 2018. Association between polycyclic aromatic hydrocarbon exposure and peripheral blood mononuclear cell DNA damage in human volunteers during fire extinction exercises. Mutagenesis 33, 105–115. https://doi.org/10.1093/MUTAGE/GEX021.

Atale, N., Gupta, S., Yadav, U.C.S., Rani, V., 2014. Cell-death assessment by fluorescent and nonfluorescent cytosolic and nuclear staining techniques. J. Microsc. 255, 7–19. https://doi.org/10.1111/JMI.12133.

Atia, A., Abdullah, A., 2020. NQO1 enzyme and its role in cellular protection. Insight. https://doi.org/10.5281/ZENODO.3877528.

Azqueta, A., Collins, A.R., 2013. The essential comet assay: a comprehensive guide to measuring DNA damage and repair. Arch. Toxicol. 87, 949–968. https://doi.org/10.1007/S00204-013-1070-0.

Azqueta, A., Ladeira, C., Giovannelli, L., Boutet-Robinet, E., Bonassi, S., Neri, M., Gajski, G., Duthie, S., Del Bo', C., Riso, P., Koppen, G., Basaran, N., Collins, A., Møller, P., 2020. Application of the comet assay in human biomonitoring: an hCOMET perspective. Mutat. Res., Rev. Mutat. Res. 783, 108288. https://doi.org/10.1016/J.MRREV.2019.108288.

Azqueta, A., Langie, S.A.S., Boutet-Robinet, E., Duthie, S., Ladeira, C., Møller, P., Collins, A.R., Godschalk, R.W.L., 2019. DNA repair as a human biomonitoring tool: comet assay approaches. Mutat. Res., Rev. Mutat. Res. 781, 71–87. https://doi.org/10.1016/J.MRREV.2019.03.002.

Azqueta, A., Slyskova, J., Langie, S.A.S., Gaivão, I.O.N., Collins, A., 2014. Comet assay to measure DNA repair: approach and applications. Front. Genet. 5, 288. https://doi.org/10.3389/FGENE.2014.00288.

Baralić, K., Živančević, K., Božić, D., Jennen, D., Buha Djordjevic, A., Antonijević Miljaković, E., Đukić-Ćosić, D., 2022. Potential genomic biomarkers of obesity and its comorbidities for phthalates and bisphenol A mixture: in silico toxicogenomic approach. Biocell 46, 519–533. https://doi.org/10.32604/biocell.2022.018271.

Bengtsson, Ewert, Lindblad, Joakim, Bengtsson, E., Wählby, C., Lindblad, J., 2004. Robust cell image segmentation methods robust cell image segmentation methods. Pattern Recogn. Image Anal. 14 (2), 157–167.

Billet, S., Abbas, I., Goff, J. Le, Verdin, A., André, V., Lafargue, P.E., Hachimi, A., Cazier, F., Sichel, F., Shirali, P., Garçon, G., 2008. Genotoxic potential of Polycyclic Aromatic Hydrocarbons-coated onto airborne Particulate Matter (PM2.5) in human lung epithelial A549 cells. Cancer Lett. 270, 144–155. https://doi.org/10.1016/J.CANLET.2008.04.044.

Bonassi, S., Milić, M., Neri, M., 2016. Frequency of micronuclei and other biomarkers of DNA damage in populations exposed to dusts, asbestos and other fibers. A systematic review. Mutat. Res. Rev. Mutat. Res. https://doi.org/10.1016/j.mrrev.2016.05.004.

Bopp, S.K., Barouki, R., Brack, W., Dalla Costa, S., Dorne, J.L.C.M., Drakvik, P.E., Faust, M., Karjalainen, T.K., Kephalopoulos, S., van Klaveren, J., Kolossa-Gehring, M., Kortenkamp, A., Lebret, E., Lettieri, T., Nørager, S., Rüegg, J., Tarazona, J.V., Trier, X., van de Water, B., van Gils, J., Bergman, Å., 2018. Current EU research activities on combined exposure to multiple chemicals. Environ. Int. 120, 544–562. https://doi.org/10.1016/J.ENVINT.2018.07.037.

Bopp, S.K., Kienzler, A., Richarz, A.N., van der Linden, S.C., Paini, A., Parissis, N., Worth, A.P., 2019. Regulatory assessment and risk management of chemical mixtures: challenges and ways forward. Crit. Rev. Toxicol. 49, 174–189. https://doi.org/10.1080/10408444.2019.1579169;WGROUP:STRING:PUBLICATION.

Bosnjakovic, A., Eichmann, T.O., Stern, A., Rasmussen, M.A., Lovric, M., Zegura, B., 2025. Metabolomic fingerprints of PAH exposure - identifying toxicological biomarkers in dynamically cultured 3D cell spheroids. bioRxiv 10, 663939. https://doi.org/10.1101/2025.07.10.663939.

Burchiel, S.W., Luster, M.I., 2001. Signaling by environmental polycyclic aromatic hydrocarbons in human lymphocytes. Clin. Immunol. 98, 2–10. https://doi.org/10.1006/CLIM.2000.4934.

Calabrese, E.J., Mattson, M.P., 2017. How does hormesis impact biology, toxicology, and medicine? NPJ Aging Mech. Dis. 3, 1–8. https://doi.org/10.1038/S41514-017-0013-Z. SUBJMETA=2611,378,631,92;KWRD=CHEMICAL+BIOLOGY,NEURAL+AGEING.

Carero, A.D.P., Hoet, P.H.M., Verschaeve, L., Schoeters, G., Nemery, B., 2001. Genotoxic effects of carbon black particles, diesel exhaust particles, and urban air particulates and their extracts on a human alveolar epithelial cell line (A549) and a human monocytic cell line (THP-1). Environ. Mol. Mutagen. 37, 155–163. https://doi.org/10.1002/EM.1023.

Carpenter, A.E., Jones, T.R., Lamprecht, M.R., Clarke, C., Kang, I.H., Friman, O., Guertin, D.A., Chang, J.H., Lindquist, R.A., Moffat, J., Golland, P., Sabatini, D.M., 2006. CellProfiler: image analysis software for identifying and quantifying cell phenotypes. Genome Biol. 7 (10 7), R100. https://doi.org/10.1186/GB-2006-7-10-R100.

Castel, R., Tassistro, V., Claeys-Bruno, M., Malleret, L., Orsière, T., 2023. In vitro genotoxicity evaluation of PAHs in mixtures using experimental design. Toxics 11. https://doi.org/10.3390/TOXICS11050470. Page 470 11, 470.

Castorena-Torres, F., de León, M.B., Cisneros, B., Zapata-Pérez, O., Salinas, J.E., Albores, A., 2008. Changes in gene expression induced by polycyclic aromatic hydrocarbons in the human cell lines HepG2 and A549. Toxicol. Vitro 22, 411–421. https://doi.org/10.1016/j.tiv.2007.10.009.

Chen, J., Bardes, E.E., Aronow, B.J., Jegga, A.G., 2009. ToppGene Suite for gene list enrichment analysis and candidate gene prioritization. Nucleic Acids Res. 37, 305–311. https://doi.org/10.1093/nar/gkp427.

Cho, Y.Y., Kim, S., Kim, P., Jo, M.J., Park, S.-E., Choi, Y., Jung, S.M., Kang, H.J., 2025. G-Protein-Coupled receptor (GPCR) signaling and pharmacology in metabolism: physiology, mechanisms, and therapeutic potential. Biomolecules 15, 291. https://doi.org/10.3390/biom15020291.

Choi, H., Harrison, R., Komulainen, H., Delgado Saborit, J.M., 2010. Polycyclic aromatic hydrocarbons - WHO guidelines for indoor air quality: selected pollutants - NCBI bookshelf [WWW Document]. WHO. URL. https://www.ncbi.nlm.nih.gov/books/NBK138709/.

Collins, A., Koppen, G., Valdiglesias, V., Dusinska, M., Kruszewski, M., Møller, P., Rojas, E., Dhawan, A., Benzie, I., Coskun, E., Moretti, M., Speit, G., Bonassi, S., 2014. The comet assay as a tool for human biomonitoring studies: the ComNet project. Mutat. Res., Rev. Mutat. Res. 759, 27–39. https://doi.org/10.1016/J.MRREV.2013.10.001.

Collins, A., Møller, P., Gajski, G., Vodenková, S., Abdulwahed, A., Anderson, D., Bankoglu, E.E., Bonassi, S., Boutet-Robinet, E., Brunborg, G., Chao, C., Cooke, M.S., Costa, C., Costa, S., Dhawan, A., de Lapuente, J., Bo', C. Del, Dubus, J., Dusinska, M., Duthie, S.J., Yamani, N. El, Engelward, B., Gaivão, I., Giovannelli, L., Godschalk, R., Guilherme, S., Gutzkow, K.B., Habas, K., Hernández, A., Herrero, O., Isidori, M., Jha, A.N., Knasmüller, S., Kooter, I.M., Koppen, G., Kruszewski, M., Ladeira, C., Laffon, B., Larramendy, M., Hégarat, L. Le, Lewies, A., Lewinska, A., Liwszyc, G.E., de Cerain, A.L., Manjanatha, M., Marcos, R., Milić, M., de Andrade, V.M., Moretti, M., Muruzabal, D., Novak, M., Oliveira, R., Olsen, A.K., Owiti, N., Pacheco, M., Pandey, A.K., Pfuhler, S., Pourrut, B., Reisinger, K., Rojas, E., Rundén-Pran, E., Sanz-Serrano, J., Shaposhnikov, S., Sipinen, V., Smeets, K., Stopper, H., Teixeira, J.P., Valdiglesias, V., Valverde, M., van Acker, F., van Schooten, F.J., Vasquez, M., Wentzel, J.F., Wnuk, M., Wouters, A., Žegura, B., Zikmund, T., Langie, S.A.S., Azqueta, A., 2023. Measuring DNA modifications with the comet assay: a compendium of protocols. Nat. Protoc. 18 (3 18), 929–989. https://doi.org/10.1038/s41596-022-00754-y.

Davis, A.P., Grondin, C.J., Johnson, R.J., Sciaky, D., McMorran, R., Wiegers, J., Wiegers, T.C., Mattingly, C.J., 2019. The comparative toxicogenomics database: update 2019. Nucleic Acids Res. 47, D948–D954. https://doi.org/10.1093/nar/gky868.

Denison, M.S., Nagy, S.R., 2003. Activation of the aryl hydrocarbon receptor by structurally diverse exogenous and endogenous chemicals. Annu. Rev. Pharmacol. Toxicol. 43, 309–334. https://doi.org/10.1146/ANNUREV.PHARMTOX.43.100901.135828/CITE/REFWORKS.

Dinkova-Kostova, A.T., Talalay, P., 2010. NAD(P)H:quinone acceptor oxidoreductase 1 (NQO1), a multifunctional antioxidant enzyme and exceptionally versatile cytoprotector. Arch. Biochem. Biophys. 501, 116–123. https://doi.org/10.1016/j.abb.2010.03.019.

Dong, C. Di, Tsai, M.L., Wang, T.H., Chang, J.H., Chen, C.W., Hung, C.M., 2020. Removal of polycyclic aromatic hydrocarbon (PAH)-contaminated sediments by persulfate oxidation and determination of degradation product cytotoxicity based on HepG2 and ZF4 cell lines. Environ. Sci. Pollut. Control Ser. 27, 34596–34605. https://doi.org/10.1007/S11356-019-04421-W/FIGURES/5.

Dong, H., Shertzer, H.G., Genter, M.B., Gonzalez, F.J., Vasiliou, V., Jefcoate, C., Nebert, D.W., 2013. Mitochondrial targeting of mouse NQO1 and CYP1B1 proteins. Biochem. Biophys. Res. Commun. 435, 727–732. https://doi.org/10.1016/J.BBRC.2013.05.051.

Duan, H., Leng, S., Pan, Z., Dai, Y., Niu, Y., Huang, C., Bin, P., Wang, Y., Liu, Q., Chen, W., Zheng, Y., 2009. Biomarkers measured by cytokinesis-block micronucleus cytome assay for evaluating genetic damages induced by polycyclic aromatic hydrocarbons. Mutat. Res., Genet. Toxicol. Environ. Mutagen. 677, 93–99. https://doi.org/10.1016/J.MRGENTOX.2009.06.002.

European Chemicals Agency, 2026. Occupational exposure limits [WWW Document]. URL. https://echa.europa.eu/oel.

European Commission, 2026. Proposal for a Directive of the European Parliament and of the Council amending Directive 2004/37/EC as regards the addition of substances and setting limit values in its Annexes I, III and IIIa [WWW Document]. URL. https://eur-lex.europa.eu/legal-content/EN/TXT/HTML/?uri=CELEX:52025PC0418.

Ewa, B., Danuta, M.Š., 2017. Polycyclic aromatic hydrocarbons and PAH-related DNA adducts. J. Appl. Genet. 58, 321–330. https://doi.org/10.1007/S13353-016-0380-3/TABLES/1.

Fenech, M., 2007. Cytokinesis-block micronucleus cytome assay. Nat. Protoc. 2 (5 2), 1084–1104. https://doi.org/10.1038/nprot.2007.77.

Fenech, M., 2020. Cytokinesis-block micronucleus cytome assay evolution into a more comprehensive method to measure chromosomal instability. Genes. https://doi.org/10.3390/genes11101203.

Fenech, M., Kirsch-Volders, M., Natarajan, A.T., Surralles, J., Crott, J.W., Parry, J., Norppa, H., Eastmond, D.A., Tucker, J.D., Thomas, P., 2011. Molecular mechanisms of micronucleus, nucleoplasmic bridge and nuclear bud formation in mammalian and human cells. Mutagenesis 26, 125–132. https://doi.org/10.1093/MUTAGE/GEQ052.

Fenech, M., Knasmueller, S., Bolognesi, C., Holland, N., Bonassi, S., Kirsch-Volders, M., 2020. Micronuclei as biomarkers of DNA damage, aneuploidy, inducers of chromosomal hypermutation and as sources of pro-inflammatory DNA in humans. Mutat. Res. Rev. Mutat. Res. 786. https://doi.org/10.1016/J.MRREV.2020.108342.

Fernández-Bertólez, N., Brandão, F., Costa, C., Pásaro, E., Teixeira, J.P., Laffon, B., Valdiglesias, V., 2021. Suitability of the in vitro cytokinesis-block micronucleus test for genotoxicity assessment of tio2 nanoparticles on sh-sy5y cells. Int. J. Mol. Sci. 22, 8558. https://doi.org/10.3390/IJMS22168558/S1.

Flusberg, D.A., Sorger, P.K., 2015. Surviving apoptosis: life-death signaling in single cells. Trends Cell Biol. 25, 446. https://doi.org/10.1016/J.TCB.2015.03.003.
Foster, K.A., Oster, C.G., Mayer, M.M., Avery, M.L., Audus, K.L., 1998. Characterization of the A549 cell line as a type II pulmonary epithelial cell model for drug metabolism. Exp. Cell Res. 243, 359–366. https://doi.org/10.1006/EXCR.1998.4172.
Gajski, G., Gerić, M., 2022. Cytogenetic methods for measuring effects of occupational exposure. In: Madalena Marques de Oliveira, M., Barreira Morais, S., Pinto Lisboa Martins Rodrigues, F. (Eds.), An Essential Guide to Occupational Exposure. Nova Science Publishers, pp. 129–165. https://doi.org/10.52305/VGMC6738.
Gajski, G., Gerić, M., Nikolić, M., Matković, K., Kazensky, L., Milić, M., 2026. Micronucleus assay in human lymphocytes and exfoliated buccal cells. Methods Mol. Biol. 2986, 171–197. https://doi.org/10.1007/978-1-0716-4976-3_9.
Gajski, G., Gerić, M., Žegura, B., Novak, M., Nunić, J., Bajrektarević, D., Garaj-Vrhovac, V., Filipič, M., 2016. Genotoxic potential of selected cytostatic drugs in human and zebrafish cells. Environ. Sci. Pollut. Control Ser. 23, 14739–14750. https://doi.org/10.1007/S11356-015-4592-6/TABLES/3.
Gajski, G., Kašuba, V., Milić, M., Gerić, M., Matković, K., Delić, L., Nikolić, M., Pavičić, M., Rozgaj, R., Garaj-Vrhovac, V., Kopjar, N., 2024. Exploring cytokinesis block micronucleus assay in Croatia: a journey through the past, present, and future in biomonitoring of the general population. Mutat. Res., Genet. Toxicol. Environ. Mutagen. 895, 503749. https://doi.org/10.1016/J.MRGENTOX.2024.503749.
Gajski, G., Ladeira, C., Gerić, M., Garaj-Vrhovac, V., Viegas, S., 2018. Genotoxicity assessment of a selected cytostatic drug mixture in human lymphocytes: a study based on concentrations relevant for occupational exposure. Environ. Res. 161, 26–34. https://doi.org/10.1016/j.envres.2017.10.044.
Gajski, G., Langie, S., Zhanataev, A., 2020. Recent applications of the Comet Assay: a report from the International Comet Assay Workshop 2019. Toxicol. Lett. 333, 1–3. https://doi.org/10.1016/J.TOXLET.2020.07.022.
Gaskill, S.J., Bruce, E.D., 2016. Binary mixtures of polycyclic aromatic hydrocarbons display nonadditive mixture interactions in an in vitro liver cell model. Risk Anal. 36, 968–991. https://doi.org/10.1111/RISA.12475.
Genies, C., Maître, A., Lefèbvre, E., Jullien, A., Chopard-Lallier, M., Douki, T., 2013. The extreme variety of genotoxic response to benzo[a]pyrene in three different human cell lines from three different organs. PLoS One 8, e78356. https://doi.org/10.1371/journal.pone.0078356.
Gminski, R., Tang, T., Mersch-Sundermann, V., 2010. Cytotoxicity and genotoxicity in human lung epithelial A549 cells caused by airborne volatile organic compounds emitted from pine wood and oriented strand boards. Toxicol. Lett. 196, 33–41. https://doi.org/10.1016/J.TOXLET.2010.03.015.
Godrèche, C., Kostov, I., Yekutieli, I., 1992. Topological correlations in cellular structures and planar graph theory. Phys. Rev. Lett. 69, 2674. https://doi.org/10.1103/PhysRevLett.69.2674.
Grishanova, A.Y., Perepechaeva, M.L., 2022. Aryl hydrocarbon receptor in oxidative stress as a double agent and its biological and therapeutic significance. Int. J. Mol. Sci. https://doi.org/10.3390/ijms23126719.
Hartiala, M., Elenius, V., Pesquera, A.A., Androulakis, S., Annesi-Maesano, I., Badyda, A., Brandsma, S., Chatziprodromidou, I., Gajski, G., Garcia-Aymerich, J., Giorio, C., Hugg, T., Jaakkola, J.J.K., Koch, S., Leonards, P.E.G., Matrali, A., Melymuk, L., Mueller, N., Muszyński, A., Opbroek, J., Paciência, I., Pandis, S.N., Pozdniakova, S., Rantala, A.K., Sufuentes, S.R., Schenk, L., Sugeng, E., Sunyer-Caldú, A., Vantarakis, A., Zherebker, A., Alfaro-Moreno, E., Nizzetto, P.B., Dominguez, J.F., Karatzas, S., Mureddu, F., Salonen, H., Papadopoulos, N., Jartti, T., 2025. Exposures in indoor air affecting health. Allergy: Europ. J. Allergy Clin. Immunol. 0 4. https://doi.org/10.1111/all.70179.
Hayes, A.W., Li, R., Hoeng, J., Iskandar, A., Peistch, M.C., Dourson, M.L., 2019. New approaches to risk assessment of chemical mixtures. Toxicol. Res. Appl. 3. https://doi.org/10.1177/2397847318820768.
Heid, S.E., Pollenz, R.S., Swanson, H.I., 2000. Role of heat shock protein 90 dissociation in mediating agonist-induced activation of the aryl hydrocarbon receptor. Mol. Pharmacol. 57, 82–92. https://doi.org/10.1016/S0026-895X(24)26445-2.
Hu, J., Bao, Y., Huang, H., Zhang, Z., Chen, F., Li, L., Wu, Q., 2021. The preliminary investigation of potential response biomarkers to PAHs exposure on childhood asthma. J. Expo. Sci. Environ. Epidemiol. 32 (1 32), 82–93. https://doi.org/10.1038/s41370-021-00334-4.
Hukkanen, J., Lassila, A., Päivärinta, K., Valanne, S., Sarpo, S., Hakkola, J., Pelkonen, O., Raunio, H., 2000. Induction and regulation of xenobiotic-metabolizing cytochrome P450s in the human A549 lung adenocarcinoma cell line. Am. J. Respir. Cell Mol. Biol. 22, 360–366. https://doi.org/10.1165/AJRCMB.22.3.3845.
International Agency for Research on Cancer (IARC) Working Group on the Evaluation of Carcinogenic Risks to Humans, 2010. Some non-heterocyclic polycyclic aromatic hydrocarbons and some related exposures. IARC Monogr. Eval. Carcinog. Risks Hum./World Health Org, Int. Agen. Res. Cancer 92, 1–853.
Jakovljević, I., Pehnec, G., Vađić, V., Čačković, M., Tomašić, V., Jelinić, J.D., 2018. Polycyclic aromatic hydrocarbons in PM10, PM2.5 and PM1 particle fractions in an urban area. Air Qual. Atmos. Health 11, 843–854. https://doi.org/10.1007/s11869-018-0603-3.
Jakovljević, I., Štrukil, Z.S., Godec, R., Bešlić, I., Davila, S., Lovrić, M., Pehnec, G., 2020. Pollution sources and carcinogenic risk of PAHs in PM1 particle fraction in an urban area. Int. J. Environ. Res. Publ. Health 17. https://doi.org/10.3390/IJERPH17249587. Page 9587 17, 9587.
Jakšić, D., Puel, O., Canlet, C., Kopjar, N., Kosalec, I., Klarić, M.S., 2012. Cytotoxicity and genotoxicity of versicolorins and 5- methoxysterigmatocystin in A549 cells. Arch. Toxicol. 86, 1583–1591. https://doi.org/10.1007/S00204-012-0871-X/FIGURES/2.
Jang, T.W., Kim, Y., Won, J.U., Lee, J.S., Song, J., 2018. The standards for recognition of occupational cancers related with polycyclic aromatic hydrocarbons (PAHs) in Korea. Ann. Occup. Environ. Med. 30, 13. https://doi.org/10.1186/S40557-018-0224-1.
Jiang, G., Song, X., Xie, J., Shi, T., Yang, Q., 2023. Polycyclic aromatic hydrocarbons (PAHs) in ambient air of Guangzhou city: exposure levels, health effects and cytotoxicity. Ecotoxicol. Environ. Saf. 262, 115308. https://doi.org/10.1016/J.ECOENV.2023.115308.
Jugan, M.L., Barillet, S., Simon-Deckers, A., Herlin-Boime, N., Sauvaigo, S., Douki, T., Carriere, M., 2012. Titanium dioxide nanoparticles exhibit genotoxicity and impair DNA repair activity in A549 cells. Nanotoxicology 6, 501–513. https://doi.org/10.3109/17435390.2011.587903.
Kazensky, L., Matković, K., Gerić, M., Žegura, B., Pehnec, G., Gajski, G., 2024. Impact of indoor air pollution on DNA damage and chromosome stability: a systematic review. Arch. Toxicol. https://doi.org/10.1007/s00204-024-03785-4.
Kelly, J.M., Ivatt, P.D., Evans, M.J., Kroll, J.H., Hrdina, A.I.H., Kohale, I.N., White, F.M., Engelward, B.P., Selin, N.E., 2021. Global cancer risk from unregulated polycyclic aromatic hydrocarbons. GeoHealth 5. https://doi.org/10.1029/2021GH000401.
Kim, K.H., Jahan, S.A., Kabir, E., Brown, R.J.C., 2013. A review of airborne polycyclic aromatic hydrocarbons (PAHs) and their human health effects. Environ. Int. 60, 71–80. https://doi.org/10.1016/j.envint.2013.07.019.
Kraus, O.Z., Frey, B.J., 2016. Computer vision for high content screening. Crit. Rev. Biochem. Mol. Biol. 51, 102–109. https://doi.org/10.3109/10409238.2015.1135868;JOURNAL:JOURNAL:IBMG18;WGROUP:STRING:PUBLICATION.
Kwon, Y.-J., Shin, S., Chun, Y.-J., 2021. Biological roles of cytochrome P450 1A1, 1A2, and 1B1 enzymes. Arch Pharm. Res. (Seoul) 44, 63–83. https://doi.org/10.1007/s12272-021-01306-w.
Ladeira, C., Møller, P., Giovannelli, L., Gajski, G., Haveric, A., Eyluel Bankoglu, E., Azqueta, A., Gerić, M.G., Stopper, H., Cabêda, J., Tonin, F.S., Collins, A., 2024. The comet assay as a tool in human biomonitoring studies of environmental and occupational exposure to chemicals—A systematic scoping review. Toxics 12. https://doi.org/10.3390/TOXICS12040270. Page 270 12, 270.
Låg, M., Øvrevik, J., Refsnes, M., Holme, J.A., 2020. Potential role of polycyclic aromatic hydrocarbons in air pollution-induced non-malignant respiratory diseases. Respir. Res. 21 (1 21), 1–22. https://doi.org/10.1186/S12931-020-01563-1.
Langie, S.A.S., Azqueta, A., Collins, A.R., 2015. The comet assay: past, present, and future. Front. Genet. 6, 266. https://doi.org/10.3389/FGENE.2015.00266.
Lelieveld, J., Haines, A., Burnett, R., Tonne, C., Klingmüller, K., Münzel, T., Pozzer, A., 2023. Air pollution deaths attributable to fossil fuels: observational and modelling study. BMJ 383. https://doi.org/10.1136/BMJ-2023-077784.
Li, H., Yin, N., Yang, R., Faiola, F., 2024. Advancing environmental toxicology in vitro: from immortalized cancer cell lines to 3D models derived from stem cells. Environ. Health (Lond.) 2, 332–349. https://doi.org/10.1021/ENVHEALTH.3C00199/SUPPL_FILE/EH3C00199_SI_001.PDF.
Lovrić, M., Gajski, G., Fernández-Agüera, J., Pöhlker, M., Gursch, H., Lovrić, M., Switters, J., Borg, A., Mureddu, F., Auguštin, D.H., Šunić, I., Šarac, J., Žebec, M.S., Dodigović, L., Bošnjaković, A., Karlović, N., Gajski, G., Gerić, M., Milić, M., Kašuba, V., Kazensky, L., Matković, K., Breljak, D., Madunić, I.V., Micek, V., Pehnec, G., Davila, S., Jakovljević, I., Smoljo, I., Horvat, T., Štefiček, M.J.L., Bituh, T., Žužul, S., Zauner, B., Račić, N., Fernández-Agüera, J., Domínguez-Amarillo, S., Sánchez-Muñoz, M., Pöhlker, M., Tönisson, L., Madueño, L., Düsing, S., Alas, H.D., Gursch, H., Dirry, L., Časni, K., Tran, H., Paulusberger, E., Michl, K., Cernava, T., Piškor, A., Sabljak, D., Lipej, M., Banić, I., Turkalj, M., Byčenkienė, S., Davulienė, L., Uogintė, I., Žegura, B., Novak, M., Štern, A., Kološa, K., Štampar, M., Forsmann, M., Rasmussen, M.A., Thorsen, J., Bønnelykke, K., Stokholm, J., Avino, P., Notardonato, I., Preden, J.S., Kuusk, K., Thalfeldt, M., Kuivjõgi, H., Battaglia, A., Battaglia, I., Cipriano, P., Bianchi, N.C., Forconi, M., Strbad, D., Petrić, V., Jalušić, D., Terzić, T., Terzić, I., Karanasiou, G., Demestichas, P., Borg, A., Switters, J., Mureddu, F., 2025. Evidence-driven indoor air quality improvement: an innovative and interdisciplinary approach to improving indoor air quality. Biofactors 51, e2126. https://doi.org/10.1002/BIOF.2126. CTYPE:STRING:JOURNAL.
Lovrić, M., Račić, N., Pehnec, G., Horvat, T., Lovrić Štefiček, M.J., Jakovljević, I., 2024. Indoor polycyclic aromatic hydrocarbons—relationship to ambient air, risk estimation, and source apportionment based on household measurements. Atmosphere 15. https://doi.org/10.3390/ATMOS15121525. Page 1525 15, 1525.
Lund, A.W., Bilgin, C.C., Hasan, M.A., McKeen, L.M., Stegemann, J.P., Yener, B., Zaki, M. J., Plopper, G.E., 2009. Quantification of spatial parameters in 3D cellular constructs using graph theory. BioMed Res. Int. 2009, 928286. https://doi.org/10.1155/2009/928286.
Madunić, J., Hercog, K., Gerić, M., Domijan, A.M., Žegura, B., Gajski, G., 2022. Marine toxin domoic acid induces moderate toxicological response in non-target HepG2 cells. Toxicology 470. https://doi.org/10.1016/J.TOX.2022.153157.
Marino, A., Morabito, R., Remigante, A., Daraghmeh, D.N., Karaman, R., 2024. The redox process in red blood cells: balancing oxidants and antioxidants. Antioxidants 14. https://doi.org/10.3390/ANTIOX14010036. Page 36 14, 36.
Mattingly, C.J., Rosenstein, M.C., Colby, G.T., Forrest Jr, J.N., Boyer, J.L., 2006. The comparative toxicogenomics database (CTD): a resource for comparative toxicological studies. J. Exp. Zool. Comp. Exp. Biol. 305A, 689–692. https://doi.org/10.1002/jez.a.307.
Møller, P., 2018. The comet assay: ready for 30 more years. Mutagenesis 33, 1–7. https://doi.org/10.1093/MUTAGE/GEX046.
Møller, P., Azqueta, A., Boutet-Robinet, E., Koppen, G., Bonassi, S., Milić, M., Gajski, G., Costa, S., Teixeira, J.P., Costa Pereira, C., Dusinska, M., Godschalk, R., Brunborg, G., Gutzkow, K.B., Giovannelli, L., Cooke, M.S., Richling, E., Laffon, B., Valdiglesias, V., Basaran, N., Del Bo', C., Zegura, B., Novak, M., Stopper, H., Vodicka, P., Vodenkova, S., de Andrade, V.M., Sramkova, M., Gabelova, A., Collins, A., Langie, S. A.S., 2020. Minimum Information for Reporting on the Comet Assay (MIRCA):

recommendations for describing comet assay procedures and results. Nat. Protoc. 15 (12 15), 3817–3826. https://doi.org/10.1038/s41596-020-0398-1.
Møller, P., Collins, A., Rodriguez-Garraus, A., Langie, S.A.S., Godschalk, R., Azqueta, A., 2025. Slightly increased level of DNA migration in the comet assay: does statistical significance equal biological significance? Mutagenesis 40, 99–110. https://doi.org/10.1093/MUTAGE/GEAF004.
Mosmann, T., 1983. Rapid colorimetric assay for cellular growth and survival: Application to proliferation and cytotoxicity assays. J. Immunol. Methods 65, 55–63. https://doi.org/10.1016/0022-1759(83)90303-4.
Muthusamy, S., Peng, C., Ng, J.C., 2018. Genotoxicity evaluation of multi-component mixtures of polyaromatic hydrocarbons (PAHs), arsenic, cadmium, and lead using flow cytometry based micronucleus test in HepG2 cells. Mutat. Res., Genet. Toxicol. Environ. Mutagen. 827, 9–18. https://doi.org/10.1016/J.MRGENTOX.2018.01.002.
Nassikas, N.J., Horner, E., Rice, M.B., Boston, M., 2024. Paradigms and perspectives indoor air: guidelines, policies, and regulation. J. Allergy Clin. Immunol. 154, 911–913. https://doi.org/10.1016/j.jaci.2024.06.015.
Nersesyan, A., Fenech, M., Bolognesi, C., Mišík, M., Setayesh, T., Wultsch, G., Bonassi, S., Thomas, P., Knasmüller, S., 2016. Use of the lymphocyte cytokinesis-block micronucleus assay in occupational biomonitoring of genome damage caused by in vivo exposure to chemical genotoxins: past, present and future. Mutat. Res., Rev. Mutat. Res. 770, 1–11. https://doi.org/10.1016/J.MRREV.2016.05.003.
Nisbet, I.C.T., LaGoy, P.K., 1992. Toxic equivalency factors (TEFs) for polycyclic aromatic hydrocarbons (PAHs). Regul. Toxicol. Pharmacol. 16, 290–300. https://doi.org/10.1016/0273-2300(92)90009-X.
Novak, M., Žegura, B., Baebler, Š., Štern, A., Rotter, A., Stare, K., Filipič, M., 2016. Influence of selected anti-cancer drugs on the induction of DNA double-strand breaks and changes in gene expression in human hepatoma HepG2 cells. Environ. Sci. Pollut. Control Ser. 23, 14751–14761. https://doi.org/10.1007/S11356-015-5420-8/FIGURES/3.
Novak, M., Žegura, B., Modic, B., Heath, E., Filipič, M., 2017. Cytotoxicity and genotoxicity of anticancer drug residues and their mixtures in experimental model with zebrafish liver cells. Sci. Total Environ. 601–602, 293–300. https://doi.org/10.1016/J.SCITOTENV.2017.05.115.
OECD, 2022. Environment Directorate Chemicals and Biotechnology Committee Establishing Occupational Exposure Limits Series on Testing and Assessment, No. 351 JT03498004 OFDE.
OECD, 2025. Environment Directorate Chemicals and Biotechnology Committee Guiding Principles for Mixture Threshold Derivation from Effect Biomarkers Series on Testing and Assessment, No 414 JT03571914 OFDE.
Patel, A.B., Shaikh, S., Jain, K.R., Desai, C., Madamwar, D., 2020. Polycyclic aromatic hydrocarbons: sources, toxicity, and remediation approaches. Front. Microbiol. 11, 562813. https://doi.org/10.3389/FMICB.2020.562813/BIBTEX.
Peng, C., Chen, W., Liao, X., Wang, M., Ouyang, Z., Jiao, W., Bai, Y., 2011. Polycyclic aromatic hydrocarbons in urban soils of Beijing: status, sources, distribution and potential risk. Environ. Pollut. 159, 802–808. https://doi.org/10.1016/J.ENVPOL.2010.11.003.
Pleil, J.D., Ariel Geer Wallace, M., Davis, M.D., Matty, C.M., 2021. The physics of human breathing: flow, timing, volume, and pressure parameters for normal, on-demand, and ventilator respiration. J. Breath Res. 15. https://doi.org/10.1088/1752-7163/AC2589.
Račić, N., Terzić, I., Karlović, N., Bošnjaković, A., Terzić, T., Jakovljević, I., Pehnec, G., Horvat, T., Gajski, G., Gerić, M., Vitko, S., Šunić, I., Forsmann, M., Avino, P., Banić, I., Lipej, M., Malev, O., Žegura, B., Switters, J., Mureddu, F., Lovrić, M., 2025. Volatile organic compounds (VOCs) and polycyclic aromatic hydrocarbons (PAHs) in indoor environments: a review and analysis of measured concentrations in Europe. Indoor Air, 5945455. https://doi.org/10.1155/INA/5945455.
Rajpara, R.K., Dudhagara, D.R., Bhatt, J.K., Gosai, H.B., Dave, B.P., 2017. Polycyclic aromatic hydrocarbons (PAHs) at the Gulf of Kutch, Gujarat, India: occurrence, source apportionment, and toxicity of PAHs as an emerging issue. Mar. Pollut. Bull. 119, 231–238. https://doi.org/10.1016/J.MARPOLBUL.2017.04.039.
Rodríguez-Romero, I.M., Gómez Arroyo, S., Villalobos Pietrini, R., Martínez Valenzuela, C., Cortés Eslava, J., Calderón Ezquerro, M.D.C., García Martínez, R., Arenas Huertero, F., Calderón Segura, M.E., 2012. Evaluation of 8-hydroxy-2′-deoxyguanosine (8-OHdG) adduct levels and DNA strand breaks in human peripheral blood lymphocytes exposed in vitro to polycyclic aromatic hydrocarbons with or without animal metabolic activation. Toxicol. Mech. Methods 22, 170–183. https://doi.org/10.3109/15376516.2011.623330.
Rossner, P., Strapacova, S., Stolcpartova, J., Schmuczerova, J., Milcova, A., Neca, J., Vlkova, V., Brzicova, T., Machala, M., Topinka, J., 2016. Toxic effects of the major components of diesel exhaust in human alveolar basal epithelial cells (A549). Int. J. Mol. Sci. 17, 17. https://doi.org/10.3390/IJMS17091393.
Rotter, S., Beronius, A., Boobis, A.R., Hanberg, A., van Klaveren, J., Luijten, M., Machera, K., Nikolopoulou, D., van der Voet, H., Zilliacus, J., Solecki, R., 2018. Overview on legislation and scientific approaches for risk assessment of combined exposure to multiple chemicals: the potential EuroMix contribution. Crit. Rev. Toxicol. 48, 796–814. https://doi.org/10.1080/10408444.2018.1541964.
Schindelin, J., Arganda-Carreras, I., Frise, E., Kaynig, V., Longair, M., Pietzsch, T., Preibisch, S., Rueden, C., Saalfeld, S., Schmid, B., Tinevez, J.Y., White, D.J., Hartenstein, V., Eliceiri, K., Tomancak, P., Cardona, A., 2012. Fiji: an open-source platform for biological-image analysis. Nat. Methods 9 (7 9), 676–682. https://doi.org/10.1038/nmeth.2019.
Schneider, C.A., Rasband, W.S., Eliceiri, K.W., 2012. NIH image to ImageJ: 25 years of image analysis. Nat. Methods 9 (7 9), 671–675. https://doi.org/10.1038/nmeth.2089.
Shimada, T., Fujii-Kuriyama, Y., 2004. Metabolic activation of polycyclic aromatic hydrocarbons to carcinogens by cytochromes P450 1A1 and 1B1. Cancer Sci. 95, 1–6. https://doi.org/10.1111/J.1349-7006.2004.TB03162.X. JOURNAL:JOURNAL:13497006A;PAGE:STRING:ARTICLE/CHAPTER.
Smith, T.G., Lange, G.D., Marks, W.B., 1996. Fractal methods and results in cellular morphology — dimensions, lacunarity and multifractals. J. Neurosci. Methods 69, 123–136. https://doi.org/10.1016/S0165-0270(96)00080-5.
Smith, T.G., Marks, W.B., Lange, G.D., Sheriff, W.H., Neale, E.A., 1989. A fractal analysis of cell images. J. Neurosci. Methods 27, 173–180. https://doi.org/10.1016/0165-0270(89)90100-3.
Štampar, M., Sedighi Frandsen, H., Rogowska-Wrzesinska, A., Wrzesinski, K., Filipič, M., Žegura, B., 2021. Hepatocellular carcinoma (HepG2/C3A) cell-based 3D model for genotoxicity testing of chemicals. Sci. Total Environ. 755, 143255. https://doi.org/10.1016/J.SCITOTENV.2020.143255.
Štampar, M., Žegura, B., 2024. In vitro hepatic 3D cell models and their application in genetic toxicology: a systematic review. Mutat. Res., Genet. Toxicol. Environ. Mutagen. 900, 503835. https://doi.org/10.1016/J.MRGENTOX.2024.503835.
Takam, P., Schäffer, A., Laovitthayanggoon, S., Charerntantanakul, W., Sillapawattana, P., 2024. Toxic effect of polycyclic aromatic hydrocarbons (PAHs) on co-culture model of human alveolar epithelial cells (A549) and macrophages (THP-1). Environ. Sci. Eur. 36, 1–13. https://doi.org/10.1186/S12302-024-01003-7/FIGURES/4.
The National Institute for Occupational Safety and Health (NIOSH), 2014. Coal tar pitch volatiles [WWW Document]. URL. https://www.cdc.gov/niosh/idlh/65996932.html.
Tomasetig, F., Tebby, C., Graillot, V., Zeman, F., Pery, A., Cravedi, J.P., Audebert, M., 2020. Comparative genotoxic potential of 27 polycyclic aromatic hydrocarbons in three human cell lines. Toxicol. Lett. 326, 99–105. https://doi.org/10.1016/J.TOXLET.2020.03.007.
Tong, R., Yang, X., Su, H., Pan, Y., Zhang, Q., Wang, J., Long, M., 2018. Levels, sources and probabilistic health risks of polycyclic aromatic hydrocarbons in the agricultural soils from sites neighboring suburban industries in Shanghai. Sci. Total Environ. 616–617, 1365–1373. https://doi.org/10.1016/J.SCITOTENV.2017.10.179.
Valerio, L.G., Kepa, J.K., Pickwell, G.V., Quattrochi, L.C., 2001. Induction of human NAD(P)H:quinone oxidoreductase (NQO1) gene expression by the flavonol quercetin. Toxicol. Lett. 119, 49–57. https://doi.org/10.1016/S0378-4274(00)00302-7.
Wang, J.Y.J., 2019. Cell death response to DNA damage. Yale J. Biol. Med. 92, 771.
Warde-Farley, D., Donaldson, S.L., Comes, O., Zuberi, K., Badrawi, R., Chao, P., Franz, M., Grouios, C., Kazi, F., Lopes, C.T., Maitland, A., Mostafavi, S., Montojo, J., Shao, Q., Wright, G., Bader, G.D., Morris, Q., 2010. The GeneMANIA prediction server: biological network integration for gene prioritization and predicting gene function. Nucleic Acids Res. 38, W214–W220. https://doi.org/10.1093/nar/gkq537.
Wickham, H., 2016. ggplot2. Use R. https://doi.org/10.1007/978-3-319-24277-4.
World Health Organization (WHO), 2000. Air Quality Guidelines for Europe, second ed. WHO Regional Publications, European Series.
Wrzesinski, K., Fey, S.J., 2018. Metabolic reprogramming and the recovery of physiological functionality in 3D cultures in micro-bioreactors. Bioengineering 5. https://doi.org/10.3390/BIOENGINEERING5010022. Page 22 5, 22.
Zhang, F., Zhao, B., Fan, Y., Qin, L., Shi, J., Chen, L., Xu, L., Jin, X., Sun, M., Deng, H., Zeng, H., Xiao, Z., Yang, X., Ge, G., 2025. Discovery of a novel AhR–CYP1A1 axis activator for mitigating inflammatory diseases using an in situ functional imaging assay. Acta Pharm. Sin. B 15, 508–525. https://doi.org/10.1016/j.apsb.2024.09.014.
Zhang, X., Yang, L., Zhang, H., Xing, W., Wang, Y., Bai, P., Zhang, L., Hayakawa, K., Toriba, A., Wei, Y., Tang, N., 2021. Assessing approaches of human inhalation exposure to polycyclic aromatic hydrocarbons: a review. Int. J. Environ. Res. Publ. Health 18. https://doi.org/10.3390/IJERPH18063124. Page 3124 18, 3124.